

=====

“Electronic Supplementary Information (ESI) to be published electronically”

=====

FOR

**Palladium(II) complexes of *N,N*-diphenylacetamide based thio/selenoethers
and flower shaped Pd₁₆S₇ and prismatic Pd₁₇Se₁₅ nano-particles tailored as
catalysts for C–C and C–O coupling**

Poornima Singh,^a and Ajai Kumar Singh^a

^a*Department of Chemistry, Indian Institute of Technology Delhi, Hauzkhaz, New Delhi-110016, India*

E-mail address: aksingh@chemistry.iitd.ac.in

Tel : 91 (011) 25691379

Contents

Page. No.

1. Multi nuclear NMR and mass spectra of P1	Figures S1–S3	3–4
2. Multi nuclear NMR and mass spectra of L1	Figures S4–S6	5–6
3. Multi nuclear NMR of C1	Figures S7–S8	7
4. Multi nuclear NMR and mass spectra of L2	Figures S9–S12	8–9
5. Multi nuclear NMR of C2	Figures S13–S15	10–11
6. Elemental analyses of bulk sample of flower shaped Pd ₁₆ S ₇ nanoparticles	Table S1	12
7. Elemental analyses of bulk sample of prismatic Pd ₁₇ Se ₁₅ nanoparticles	Table S2	12
8. Crystal data and structural refinement parameters of P1, L1, L2, C1 & C2	Table S3	13
9. Selected bond lengths and bond angles of P1, L1, L2, C1 & C2	Table S4	14–16
10. Secondary interactions of P1, L1, C1 & C2	Figures S16–S21	16–18

11. Parametric details of weak C–H···O and C–H···Cl interactions		
	Table S5	18
12. EDX pattern of the flower shaped Pd ₁₆ S ₇ nanoparticles		
	Figures S22	19
13. EDX pattern of prismatic Pd ₁₇ Se ₁₅ nanoparticles		
	Figure S23	19
14. TEM image of NPs after 4 cycle		
	Figure S24	19
15. Proposed mechanism for Suzuki-Miyaura and C–O coupling reactions		
	Figures S25–S26	20
16. Optimization of conditions for Suzuki–Miyaura cross coupling reaction catalyzed with Pd ₁₆ S ₇ / Pd ₁₇ Se ₁₅ NPs ^a		
	Table S6	21
17. Optimization of conditions for C–O coupling reaction catalyzed with Pd ₁₆ S ₇ / Pd ₁₇ Se ₁₅ NPs ^a		
	Table S7	22
18. Optimization of base, solvent and time for Suzuki–Miyaura coupling reaction catalyzed with C1/C2		
	Table S8	23
19. Optimization of base, solvent and time for C–O coupling reaction catalyzed with C1/C2 .		
	Table S9	23
20. ‘Catalyst Alive’ Test for SMC of 4-Bromobenzaldehyde, Catalyst 0.001 mol%.		
	Figure S27	24
21. ‘Catalyst Alive’ Test for C–O Coupling of 1-Bromo-4-nitrobenzene, Catalyst 0.1 mol%		
	Figure S28	24
22. C–C and C–O coupled product NMR spectra		
	Figures S29–S41	25–31

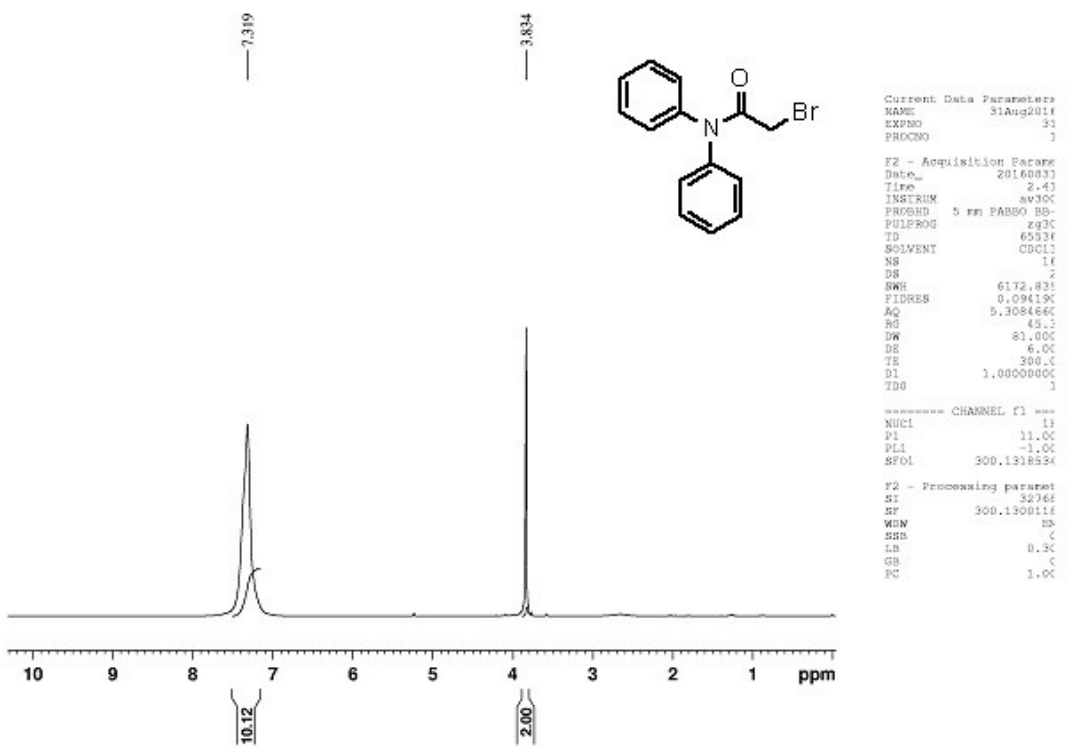


Figure S1. ^1H NMR

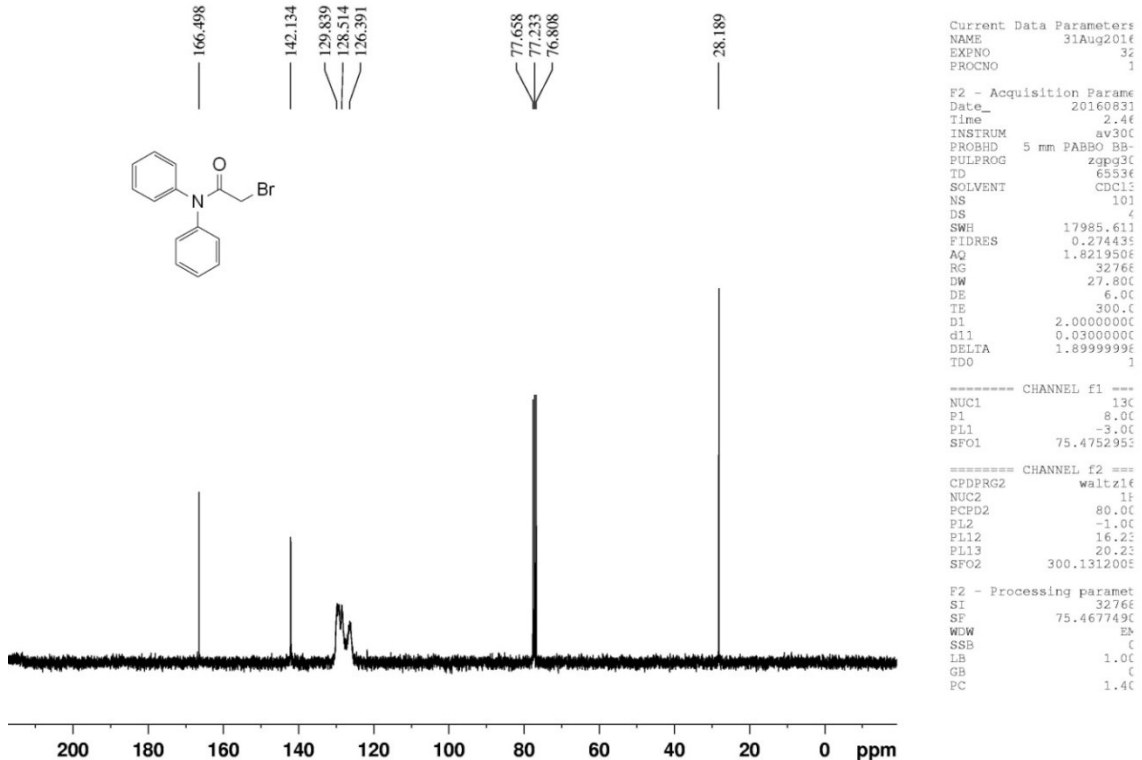


Figure S2. $^{13}\text{C}\{^1\text{H}\}$ NMR of P1

Mass Spectrum SmartFormula Report

Analysis Info

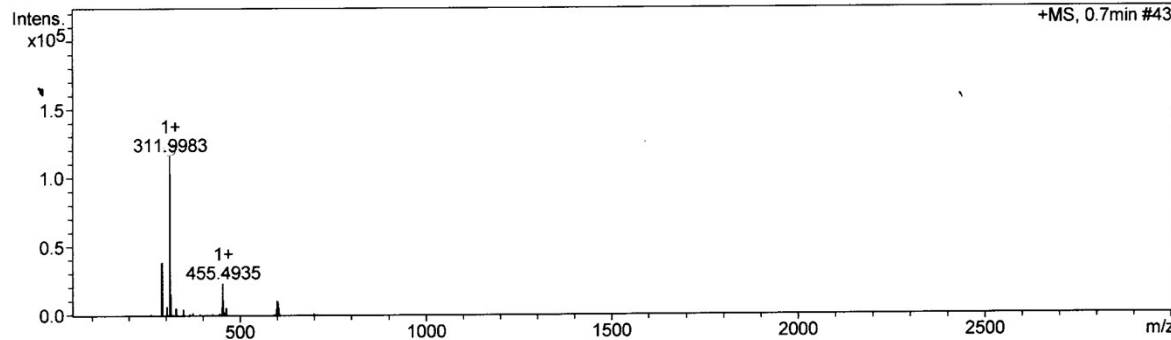
Analysis Name Z:\AUG_2016\AKS PR1.d
 Method tune_wide.m
 Sample Name
 Comment

Acquisition Date 8/1/2016 10:55:59 AM

 Operator IITD
 Instrument micrOTOF-Q II 228888.10262

Acquisition Parameter

Source Type	ESI	Ion Polarity	Positive	Set Nebulizer	0.3 Bar
Focus	Active	Set Capillary	4500 V	Set Dry Heater	180 °C
Scan Begin	50 m/z	Set End Plate Offset	-500 V	Set Dry Gas	4.0 l/min
Scan End	3000 m/z	Set Collision Cell RF	500.0 Vpp	Set Divert Valve	Source



Meas. m/z # Ion Formula	m/z	err [ppm]	Mean err [ppm]	rdb 8.5	N-Rule Conf	e ⁻	mSigm a	Std m/z	Std I Std m/z	VarNo	Std I Std m/z	Std Dev	Std Comb Dev
311.998268 1 C ₁₄ H ₁₂ BrNNaO 311.999447	3.8	3.8	8.5	ok even			42.5	30.7	1.3	8.2	1.3	842.7	

Figure S3. Mass Spectrum of P1

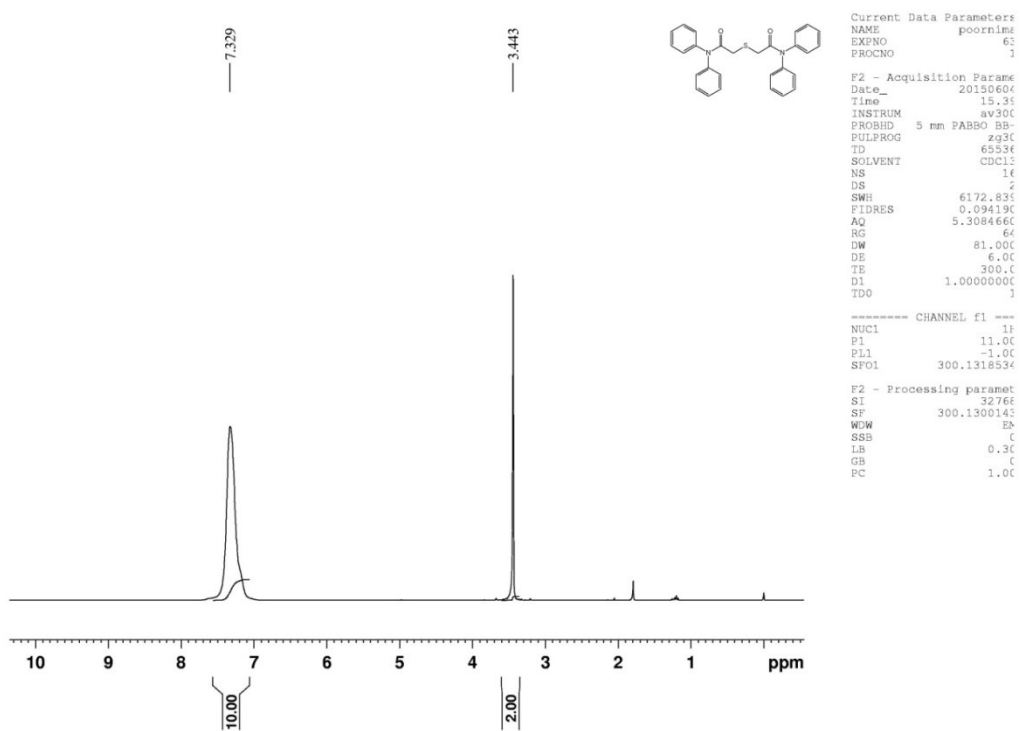


Figure S4. ^1H NMR of L1

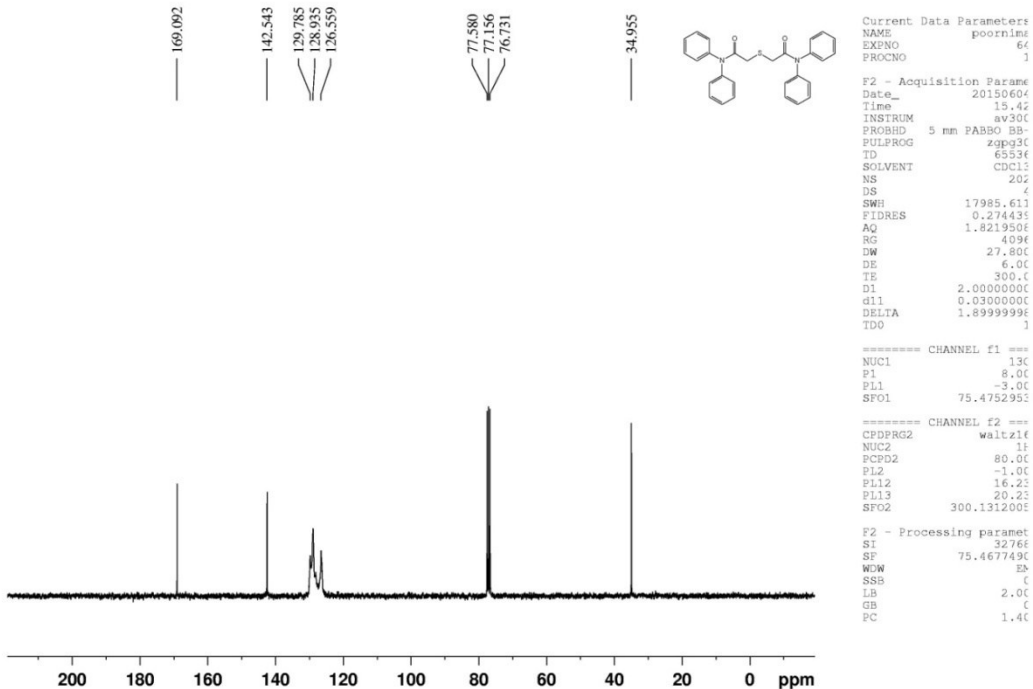


Figure S5. $^{13}\text{C}\{\text{H}\}$ NMR of L1

Mass Spectrum SmartFormula Report

Analysis Info

Analysis Name Z:\JUNE 2016\aks p1.d
 Method tune_wide.m
 Sample Name P1D
 Comment

Acquisition Date 6/27/2016 10:59:38 AM

 Operator IITD
 Instrument micrOTOF-Q II 228888.10262

Acquisition Parameter

Source Type	ESI	Ion Polarity	Positive	Set Nebulizer	0.3 Bar
Focus	Active	Set Capillary	4500 V	Set Dry Heater	180 °C
Scan Begin	50 m/z	Set End Plate Offset	-500 V	Set Dry Gas	4.0 l/min
Scan End	3000 m/z	Set Collision Cell RF	500.0 Vpp	Set Divert Valve	Source

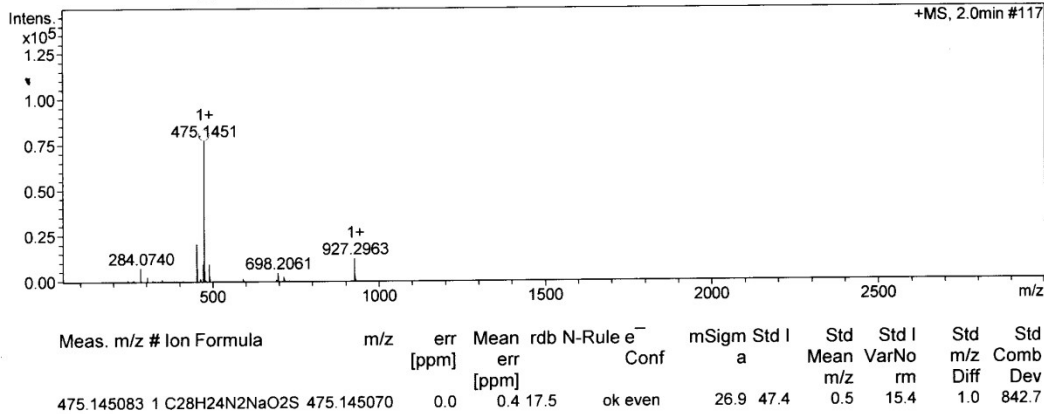


Figure S6. Mass Spectrum of L1

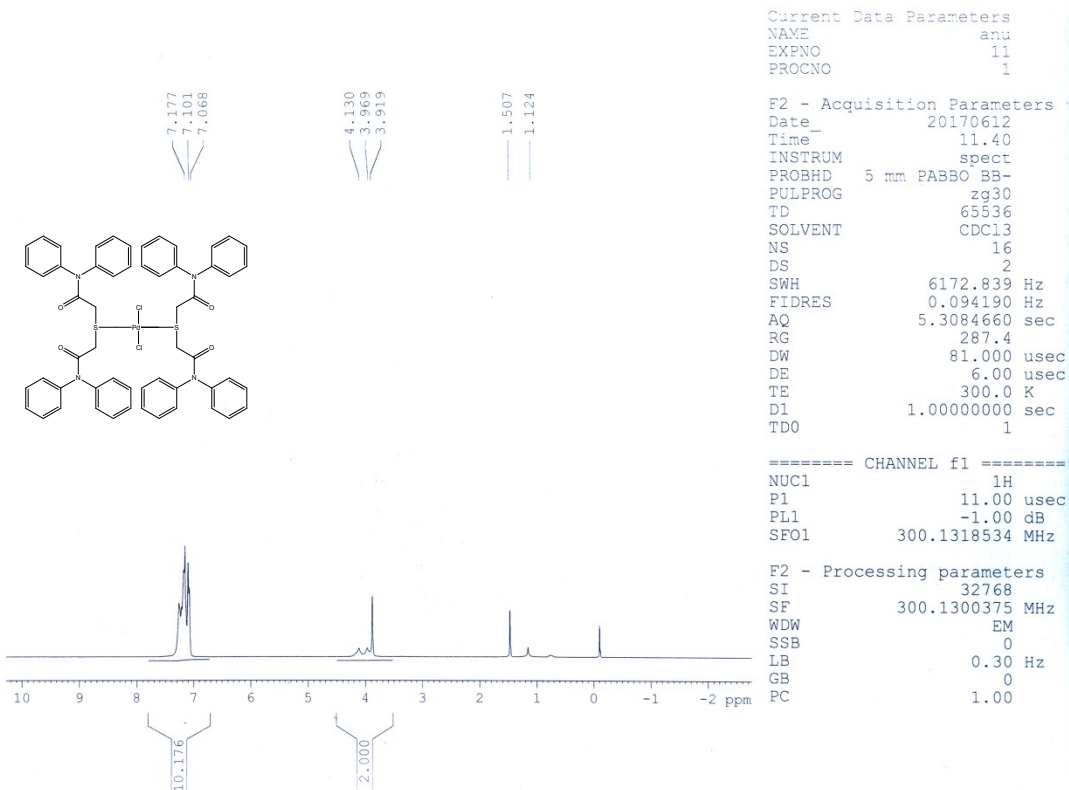


Figure S7. ¹H NMR of C1

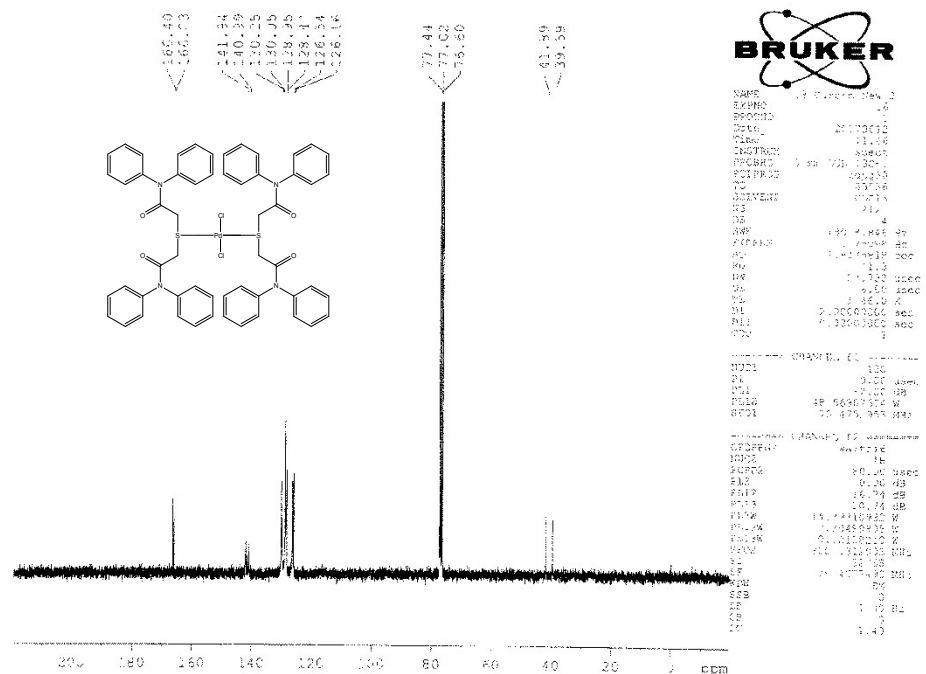


Figure S8. ¹³C{¹H} NMR of C1

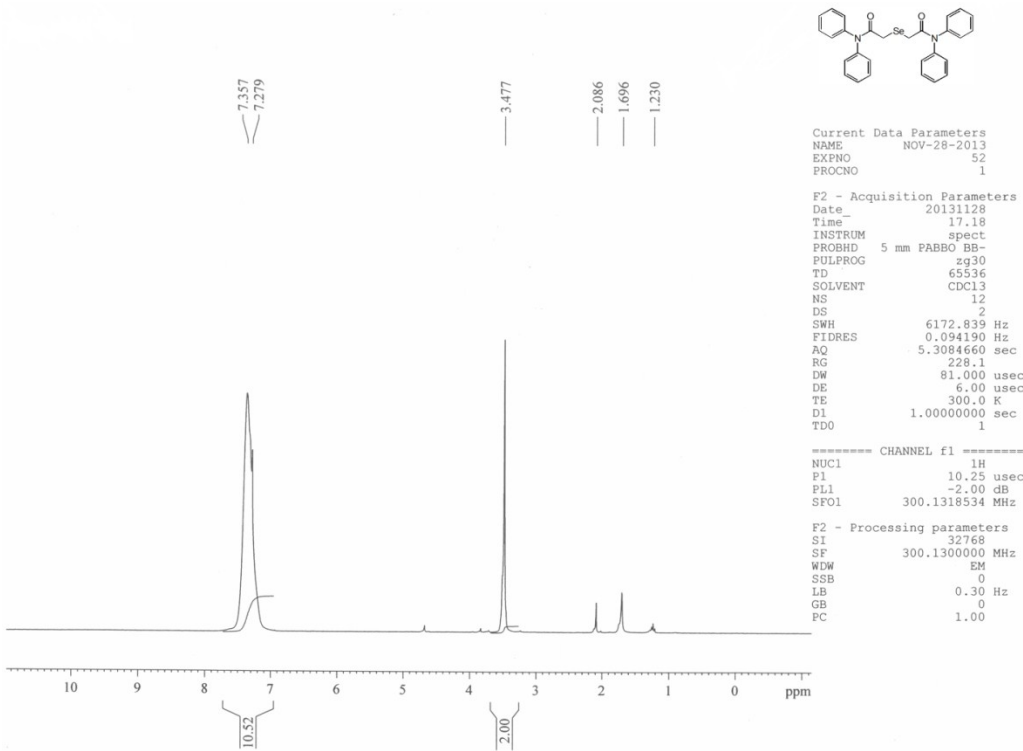


Figure S9. ¹H NMR of L2

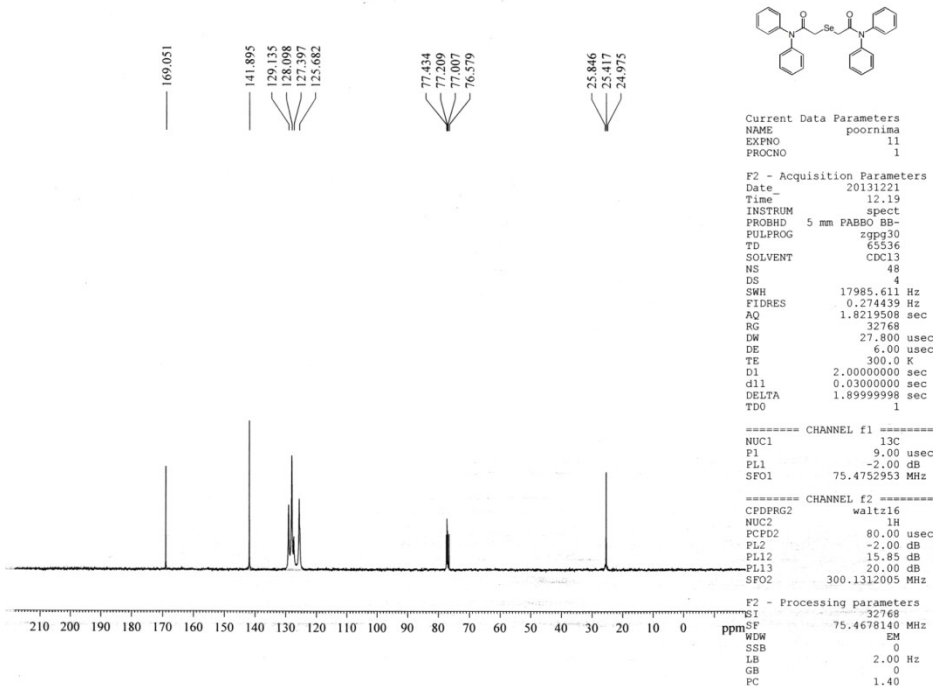


Figure S10. ¹³C{¹H} NMR of L2

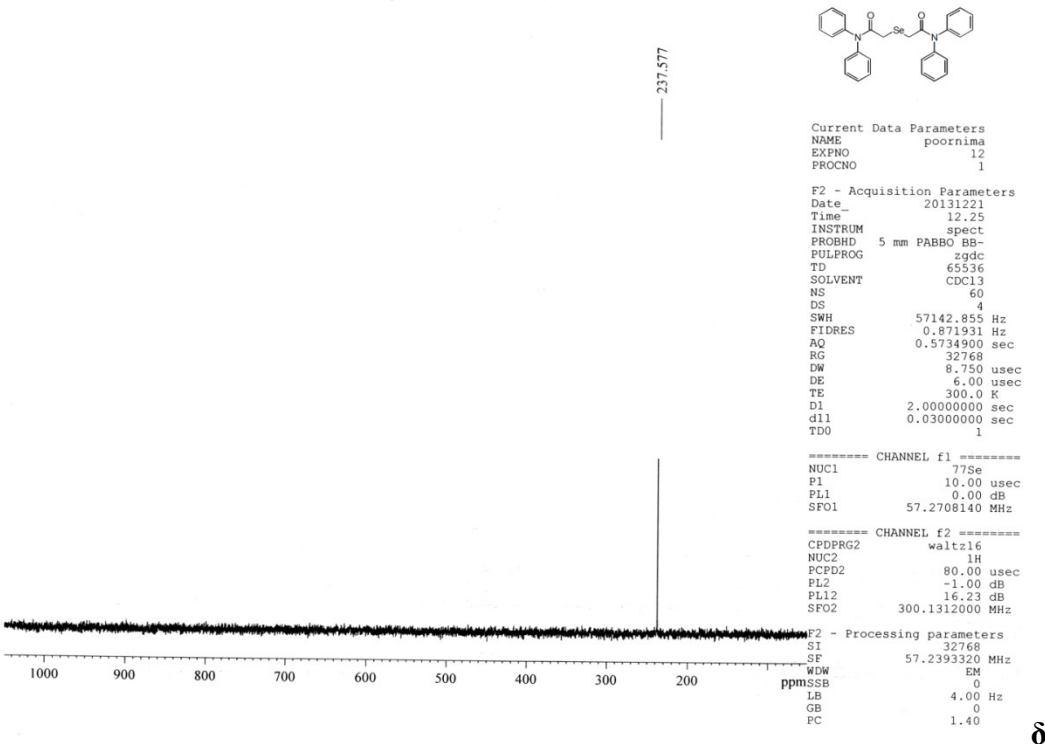


Figure S11. $^{77}\text{Se}\{\text{H}\}$ NMR of L2

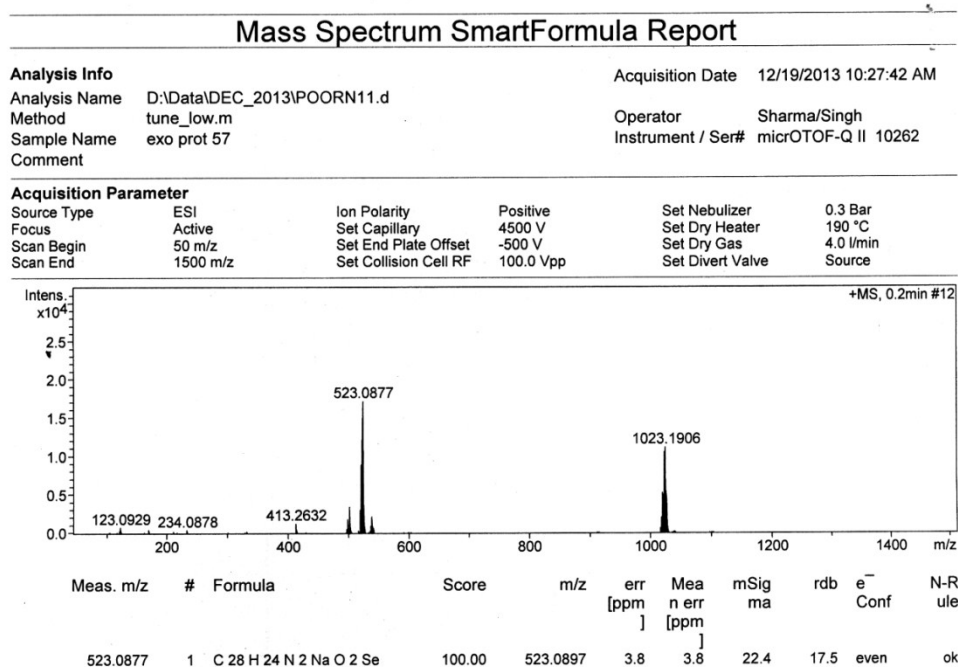


Figure S12. Mass Spectrum of L2

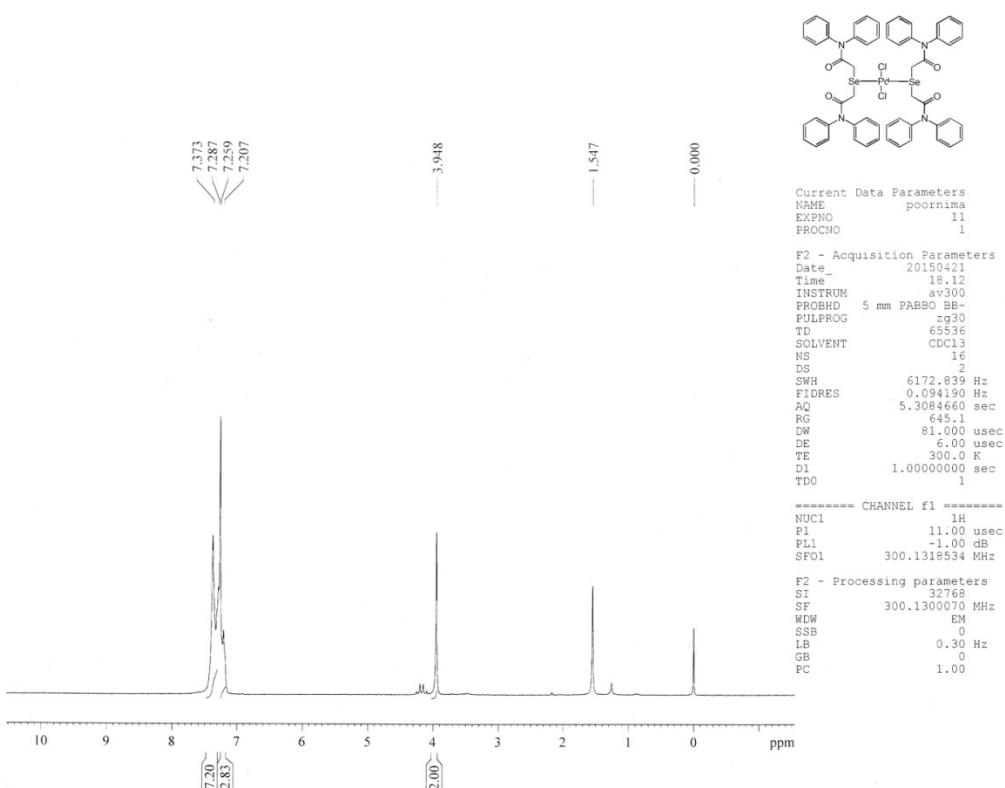


Figure S13. ^1H NMR of C2

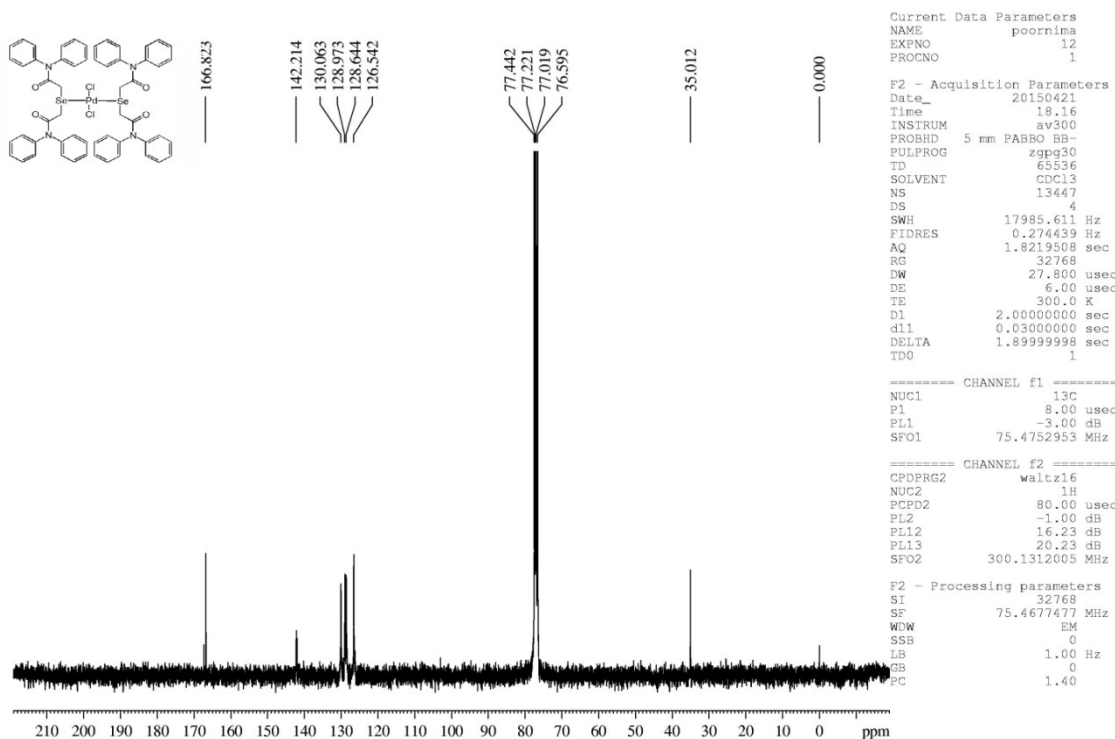


Figure S14. $^{13}\text{C}\{^1\text{H}\}$ NMR of C2

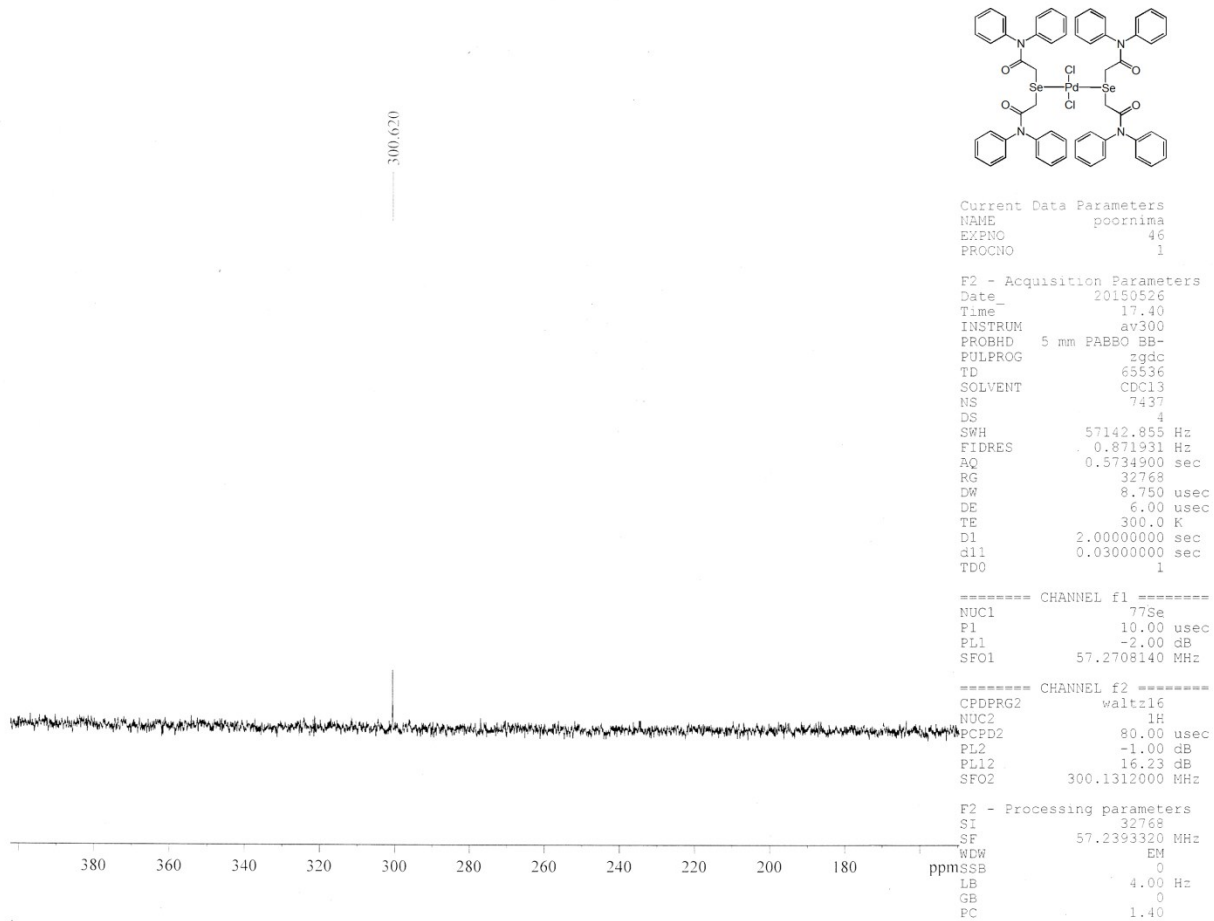


Figure S15. $^{77}\text{Se}\{\text{H}\}$ NMR C2

Table S1.**Elemental analyses of bulk sample of flower shaped Pd₁₆S₇ nanoparticles.**

Element	Weight %	Weight % σ	Atomic %
Carbon	32.602	4.281	69.1317
Nitrogen	2.3462	3.3178	4.0341
Oxygen	3.9223	1.4253	6.2331
Phosphorus	0.6396	0.1535	0.5284
Sulfur	8.6761	0.7095	7.0383
Chlorine	0.5959	0.1999	0.437
Palladium	51.2178	3.8891	12.5976

Table S2.**Elemental analyses of bulk sample of prismatic Pd₁₇Se₁₅ nanoparticles**

Element	Weight %	Weight % σ	Atomic %
Carbon	5.9232	3.5214	29.921
Nitrogen	0	0	0
Oxygen	1.1975	0.6882	4.6914
Phosphorus	0.0896	0.1092	0.1821
Chlorine	0.784	0.784	1.398
Selenium	43.5885	1.7622	34.9394
Palladium	48.4174	1.9563	28.8682

Table S3
Crystal Data and Structure Refinement Details for Precursor (P1), Ligands (L1, L2) and Complexes (C1, C2)

	P1	L1	C1	L2	C2
Empirical formula	C ₁₄ H ₁₂ BrNO	C ₂₈ H ₂₄ N ₂ O ₂ S	C ₅₆ H ₄₈ Cl ₂ N ₄ O ₄ PdS ₂ , 2(CHCl ₃)	C ₂₈ H ₂₄ N ₂ O ₂ Se	C ₅₆ H ₄₈ Cl ₂ N ₄ O ₄ PdSe ₂ , 2(C ₂ H ₃ N)
Formula mass (g mol ⁻¹)	290.15	452.55	1321.14	499.45	1258.31
Temperature (K)	298(2)	298(2)	298(2)	298(2)	298(2)
Wavelength, λ (Å)	0.71073	0.71073	0.71073	0.71073	0.71073
Crystal system	Monoclinic	Monoclinic	Triclinic	Monoclinic	Triclinic
Crystal size (mm ³)	0.29 x 0.27 x 0.25	0.33 x 0.31 x 0.28	0.31 x 0.29 x 0.27	0.32 x 0.31 x 0.29	0.33 x 0.31 x 0.29
Space group	P 2 ₁ /n	C2	P -1	P2 ₁ /n	P -1
<i>a</i> (Å)	9.398(3)	17.766(7)	11.700(4)	9.341(6)	9.430(2)
<i>b</i> (Å)	13.898(4)	5.557(2)	12.284(4)	20.608(13)	10.752(3)
<i>c</i> (Å)	10.247(3)	13.792(5)	12.639(4)	13.101(8)	14.940(4)
α (deg)	90	90	96.477(7)	90	81.965(4)
β (deg)	112.460(6)	120.633(8)	114.035(6)	109.33(1)	89.092(5)
γ (deg)	90	90	106.735(6)	90	68.046(4)
<i>V</i> (Å ³)	1236.9(6)	1171.5(8)	1532.8(9)	2380	1390.1(6)
<i>Z</i>	4	2	1	4	1
ρ_{calcd} (Mg m ⁻³)	1.558	1.283	1.431	1.394	1.503
Absorption coefficient (mm ⁻¹)	3.305	0.166	0.767	1.605	1.792
<i>F</i> (000)	584	476	672	1024	636
<i>h, k, l</i> ranges collected	-11→11	-20→20	-13→13	-11→11	-11→8
	-16→16	-6→6	-14→14	-24→24	-12→12
	-12→12	-16→16	-15→15	-15→15	-15→17
Reflection collected	11687	5687	14795	22425	5997
Independent reflections	2175 [R(int) = 0.0625]	2058 [R(int) = 0.0717]	5395 [R(int) = 0.0452]	4166 [R(int) = 0.0618]	4899 [R(int) = 0.0202]
θ range (°)	2.50–25.00	2.66–24.95	2.05–25.00	1.92–25.00	2.31–25.00
Completeness to θ_{max} (%)	99.9	99.7	99.4	99.6	98.9
Absorption correction	Semi-empirical from equivalents				
Max., min. transmission	0.432, 0.403	0.958, 0.946	0.810, 0.791	0.626, 0.602	0.598, 0.556
Refinement method	Full-matrix least-squares on F2				
Data/restraints /parameters	2173 / 0 / 154	2058 / 1 / 150	5395 / 0 / 349	4166 / 0 / 298	4504 / 0 / 341
Goodness of fit on F^2	1.024	1.082	1.108	1.010	1.023
Final <i>R</i> indices (<i>I</i> >2σ(<i>I</i>))	R1 = 0.0468, wR2 = 0.0965	R1 = 0.0804, wR2 = 0.1166	R1 = 0.0655, wR2 = 0.1624	R1 = 0.0416, wR2 = 0.0937	R1 = 0.0447, wR2 = 0.1382
<i>R</i> indices (all data)	R1 = 0.0879, wR2 = 0.1100	R1 = 0.1168, wR2 = 0.1283	R1 = 0.0771, wR2 = 0.1689	R1 = 0.0723, wR2 = 0.1137	R1 = 0.0590, wR2 = 0.1651
Largest diff peak/hole (e Å ⁻³)	0.545 / -0.465	0.292/-0.191	0.747/-0.711	0.316/-0.337	0.625 / -0.568
Extinction coefficient		—	—	—	—

Table S4**Selected bond lengths [\AA] and bond angles [$^\circ$]**

Compounds	Bond length [\AA]		Bond angle [$^\circ$]	
P1	Br(1)-C(14)	1.941(4)	C(13)-N(1)-C(6)	121.2(3)
	O(1)-C(13)	1.215(4)	C(13)-N(1)-C(7)	122.6(3)
	N(1)-C(13)	1.377(5)	C(6)-N(1)-C(7)	116.1(3)
	N(1)-C(6)	1.434(4)	C(12)-C(7)-C(8)	119.4(4)
	N(1)-C(7)	1.443(4)	C(12)-C(7)-N(1)	119.4(3)
	C(7)-C(12)	1.370(5)	C(8)-C(7)-N(1)	121.1(3)
	C(7)-C(8)	1.372(5)	C(5)-C(6)-C(1)	119.9(4)
	C(6)-C(5)	1.378(5)	C(5)-C(6)-N(1)	119.7(3)
	C(6)-C(1)	1.379(5)	C(1)-C(6)-N(1)	120.3(3)
	C(13)-C(14)	1.501(6)	O(1)-C(13)-N(1)	122.3(4)
			O(1)-C(13)-C(14)	120.1(4)
			N(1)-C(13)-C(14)	117.5(4)
			C(13)-C(14)-Br(1)	107.8(3)
L1	S(1)-C(14)	1.781(5)	C(14)-S(1)-C(14)#1	102.0(4)
	S(1)-C(14)#1	1.781(5)	C(13)-N(1)-C(7)	121.7(4)
	N(1)-C(13)	1.374(5)	C(13)-N(1)-C(2)	121.8(4)
	N(1)-C(7)	1.438(5)	C(7)-N(1)-C(2)	116.3(4)
	N(1)-C(2)	1.449(5)	O(1)-C(13)-N(1)	122.2(5)
	C(13)-O(1)	1.220(5)	O(1)-C(13)-C(14)	122.8(4)
	C(13)-C(14)	1.511(6)	N(1)-C(13)-C(14)	114.9(4)
			C(8)-C(7)-N(1)	119.6(4)
			C(12)-C(7)-N(1)	121.2(4)
			C(13)-C(14)-S(1)	115.5(3)
			C(1)-C(2)-N(1)	120.9(5)
			C(3)-C(2)-N(1)	118.6(5)
L2	Se(1)-C(14)	1.950(3)	C(14)-Se(1)-C(15)	96.99(15)
	Se(1)-C(15)	1.959(4)	O(1)-C(13)-N(1)	122.0(3)
	C(13)-O(1)	1.222(4)	O(1)-C(13)-C(14)	120.3(3)
	C(13)-N(1)	1.372(4)	N(1)-C(13)-C(14)	117.7(3)
	C(13)-C(14)	1.502(4)	C(16)-N(2)-C(17)	121.6(3)
	N(2)-C(16)	1.375(4)	C(16)-N(2)-C(23)	121.3(3)
	N(2)-C(17)	1.440(4)	C(17)-N(2)-C(23)	117.1(3)
	N(2)-C(23)	1.446(4)	C(24)-C(23)-N(2)	121.3(3)
	N(1)-C(6)	1.440(4)	C(28)-C(23)-N(2)	118.9(3)
	N(1)-C(7)	1.443(4)	C(13)-N(1)-C(6)	120.3(3)
	C(16)-O(2)	1.217(4)	C(13)-N(1)-C(7)	123.5(3)
			C(6)-N(1)-C(7)	116.1(2)
			C(8)-C(7)-N(1)	121.0(3)
			C(12)-C(7)-N(1)	119.5(3)
			C(5)-C(6)-N(1)	119.0(3)
			C(1)-C(6)-N(1)	121.4(3)
			O(2)-C(16)-N(2)	121.5(3)
			O(2)-C(16)-C(15)	120.8(3)
			N(2)-C(16)-C(15)	117.7(3)
			C(18)-C(17)-N(2)	119.1(3)
			C(22)-C(17)-N(2)	121.5(3)
			C(16)-C(15)-Se(1)	109.9(2)
			C(13)-C(14)-Se(1)	109.7(2)
C1	Pd(1)-Cl(1)#1	2.2892(15)	Cl(1)#1-Pd(1)-Cl(1)	180.000(1)
	Pd(1)-Cl(1)	2.2892(15)	Cl(1)#1-Pd(1)-S(1)	94.79(5)

	Pd(1)-S(1)	2.3235(14)	Cl(1)-Pd(1)-S(1)	85.21(5)
	Pd(1)-S(1)#1	2.3235(14)	Cl(1)#1-Pd(1)-S(1)#1	85.21(5)
	S(1)-C(14)	1.819(5)	Cl(1)-Pd(1)-S(1)#1	94.79(5)
	S(1)-C(15)	1.830(5)	S(1)-Pd(1)-S(1)#1	180.00(6)
	O(2)-C(16)	1.218(6)	C(14)-S(1)-C(15)	98.4(2)
	N(2)-C(16)	1.365(6)	C(14)-S(1)-Pd(1)	110.65(18)
	N(2)-C(23)	1.438(6)	C(15)-S(1)-Pd(1)	104.24(18)
	N(2)-C(17)	1.439(7)	C(16)-N(2)-C(23)	123.6(4)
	O(1)-C(13)	1.213(6)	C(16)-N(2)-C(17)	118.9(4)
	N(1)-C(13)	1.359(7)	C(23)-N(2)-C(17)	117.3(4)
	N(1)-C(6)	1.441(7)	C(13)-N(1)-C(6)	122.6(4)
	N(1)-C(7)	1.443(6)	C(13)-N(1)-C(7)	121.4(4)
			C(6)-N(1)-C(7)	115.9(4)
			C(16)-C(15)-S(1)	107.7(4)
			O(2)-C(16)-N(2)	123.1(5)
			O(2)-C(16)-C(15)	120.6(4)
			N(2)-C(16)-C(15)	116.2(4)
			C(5)-C(6)-N(1)	119.0(5)
			C(1)-C(6)-N(1)	120.6(5)
			C(28)-C(23)-N(2)	118.7(5)
			C(24)-C(23)-N(2)	120.4(5)
			C(13)-C(14)-S(1)	108.6(4)
			C(12)-C(7)-N(1)	119.0(5)
			C(8)-C(7)-N(1)	120.6(5)
			O(1)-C(13)-N(1)	124.3(5)
			O(1)-C(13)-C(14)	121.5(5)
			N(1)-C(13)-C(14)	114.2(5)
			C(22)-C(17)-N(2)	120.7(5)
			C(18)-C(17)-N(2)	119.9(5)
C2	C(6)-N(1)	1.438(7)	C(1)-C(6)-N(1)	121.2(5)
	C(7)-N(1)	1.420(7)	C(5)-C(6)-N(1)	117.2(5)
	C(13)-O(1)	1.234(6)	C(12)-C(7)-N(1)	119.2(5)
	C(13)-N(1)	1.361(7)	C(8)-C(7)-N(1)	120.8(5)
	C(14)-Se(1)	1.955(5)	O(1)-C(13)-N(1)	122.6(5)
	C(15)-Se(1)	1.974(5)	O(1)-C(13)-C(14)	119.0(5)
	C(16)-O(2)	1.222(6)	N(1)-C(13)-C(14)	118.4(5)
	C(16)-N(2)	1.363(7)	C(13)-C(14)-Se(1)	106.5(3)
	C(17)-N(2)	1.408(7)	C(16)-C(15)-Se(1)	107.4(3)
	C(23)-N(2)	1.449(7)	O(2)-C(16)-N(2)	120.4(5)
	C(29)-N(3)	1.086(11)	O(2)-C(16)-C(15)	122.3(5)
	Cl(1)-Pd(1)	2.2736(16)	N(2)-C(16)-C(15)	117.3(4)
	Pd(1)-Cl(1)#1	2.2736(16)	C(18)-C(17)-N(2)	121.0(5)
	Pd(1)-Se(1)	2.4151(7)	N(2)-C(17)-C(22)	120.2(5)
	Pd(1)-Se(1)#1	2.4151(7)	C(24)-C(23)-N(2)	119.4(5)
			C(28)-C(23)-N(2)	119.9(5)
			N(3)-C(29)-C(30)	175.3(14)
			C(13)-N(1)-C(7)	124.1(4)
			C(13)-N(1)-C(6)	118.5(5)
			C(7)-N(1)-C(6)	117.4(4)
			C(16)-N(2)-C(17)	120.5(4)
			C(16)-N(2)-C(23)	122.2(4)
			C(17)-N(2)-C(23)	117.0(4)
			Cl(1)-Pd(1)-Cl(1)#1	180.00(3)
			Cl(1)-Pd(1)-Se(1)	87.18(4)
			Cl(1)#1-Pd(1)-Se(1)	92.82(4)
			Cl(1)-Pd(1)-Se(1)#1	92.82(4)

		Cl(1)#1-Pd(1)-Se(1)#1	87.18(4)
		Se(1)-Pd(1)-Se(1)#1	180.0
		C(14)-Se(1)-C(15)	97.6(2)
		C(14)-Se(1)-Pd(1)	103.57(15)
		C(15)-Se(1)-Pd(1)	107.27(16)

Secondary interactions:

The intermolecular C–H···O interactions present in the crystal of **P1**, resulting supramolecular structure are shown in Fig. S16. The strong intermolecular H-bonding between O–H is present in **L2**. The centrosymmetric dimeric units that are formed *via* reciprocatory C(5)–H(5)···O2 and C(8)–H(8)···O1 H-bonding interactions, self-assemble, in the crystal lattice of **L2** as shown in Fig. S17.¹

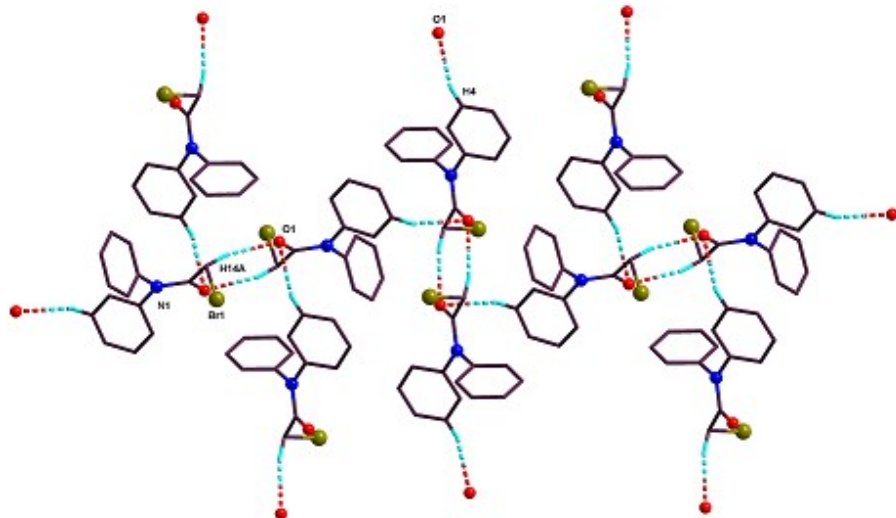


Figure S16. Supramolecular structure due to C–H···O interactions in the crystal lattice of **P1**.

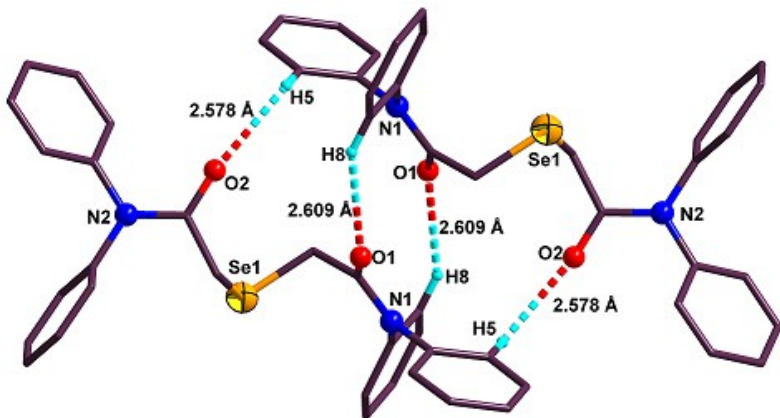


Figure S17. C–H···O interactions in the crystal lattice of **L2**.

In **C1**, intermolecular C(24)–H(24)···O2 and C(12)–H(12)···O1 H-bonding interactions result in supramolecular structure (Figs. S18 and S19). In **C2**, centrosymmetric dimeric units are formed by intermolecular C(12)–H(12)···O2 interactions in conjunction with intramolecular C(15)–H(15A)···O1, C14–H14A···Cl1 and C15–H15B···Cl1 H-bonding as shown in Fig. S20. The presence of intermolecular C(8)–H(8)···O1 interaction and intramolecular H-bonding (C(15)–H(15A)···O1), results in supramolecular structure of **C2** as shown in Figs. S20 and S21.

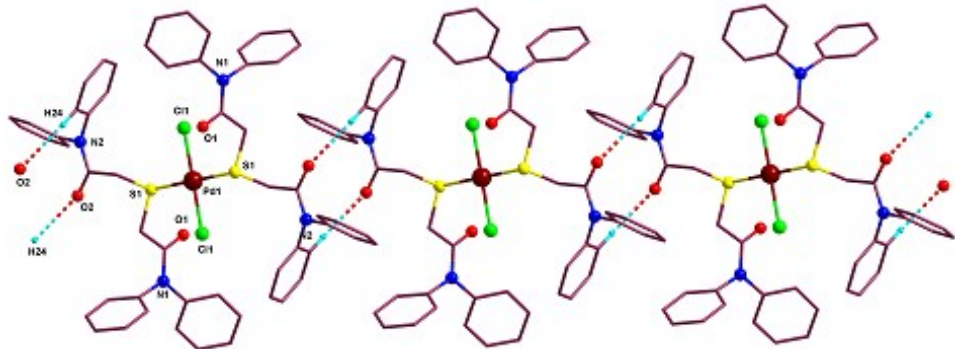


Figure S18. Supramolecular structure due to intermolecular C–H···O interactions in **C1**.

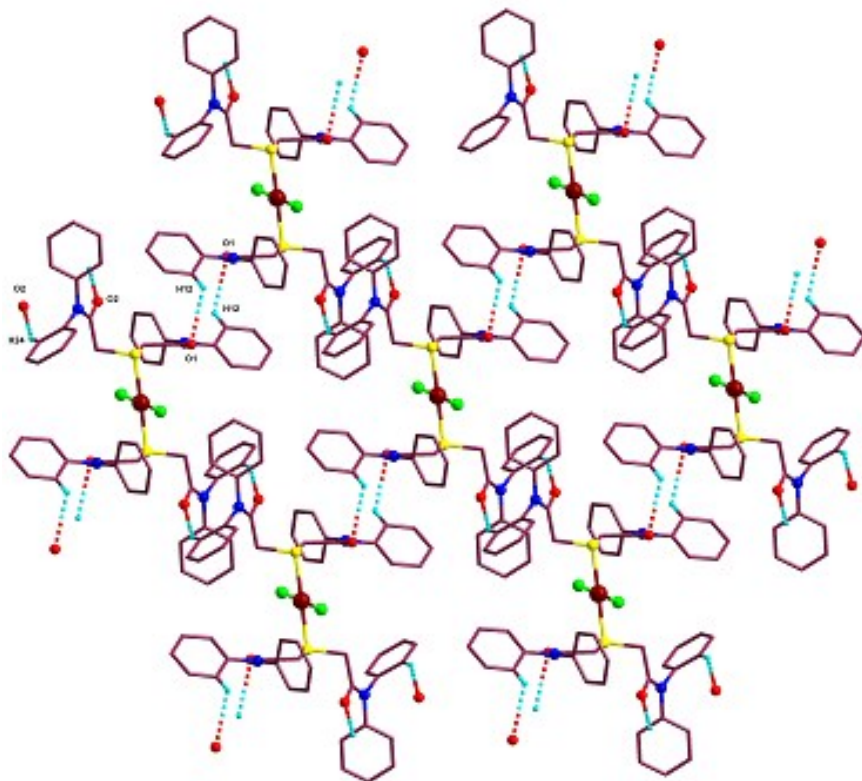


Figure S19. Supramolecular structure due to intermolecular C–H···O interactions in the crystal of **C1**.

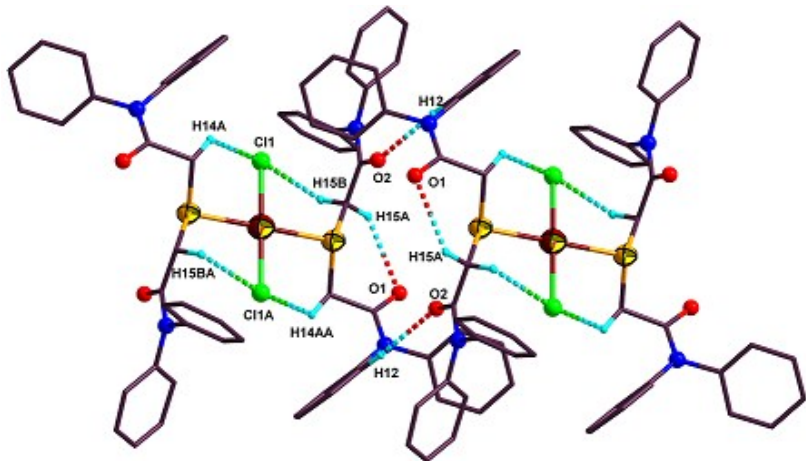


Figure S20. C–H···O and C–H···Cl interactions in the crystal lattice of **C2**.

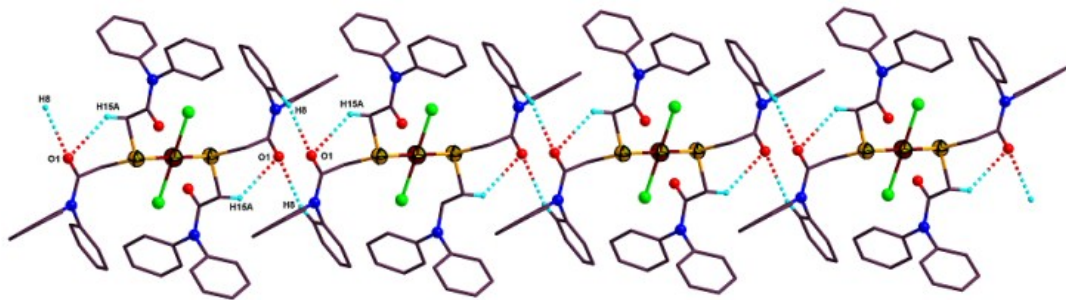


Figure S21. C–H···O interactions in the crystal of **C2**.

Table S5.

Parametric details of D–H···A interactions.

	D–H···A	d(D–H) (Å)	d(H···A) (Å)	d(D···A) (Å)	\angle (DHA) ($^{\circ}$)	Symmetry operation
P1	C(14)–H(14A)···O1	0.97	2.411	3.361(5)	166.2	2-x, -y, 2-z
	C(4)–H(4)···O1	0.93	2.666	3.340(6)	129.9	-1/2+x, 1/2-y, -1/2+z
C1	C(24)–H(24)···O2	0.93	2.617	3.450(9)	149.3	x, -1+y, z
	C(12)–H(12)···O1	0.93	2.711	3.340(8)	125.7	1+x, y, 1+z
L2	C(5)–H(5)···O2	0.93	2.578	3.257(5)	130.3	-x,-y,1-z
	C(8)–H(8)···O1	0.93	2.609	3.430(4)	147.6	-x,-y,1-z
C2	C(14)–H(14A)···Cl(1)	0.97	2.734	3.372(6)	123.8	-x,1-y,1-z
	C(15)–H(15B)···Cl(1A)	0.97	2.871	3.244(5)	103.9	-x,1-y,1-z
	C(15)–H(15A)···O(1)	0.97	2.616	3.285(6)	126.3	-x, 1-y, 1-z
	C(12)–H(12)···O(2)	0.93	2.508	3.436(9)	175.5	-x, 1-y, 1-z

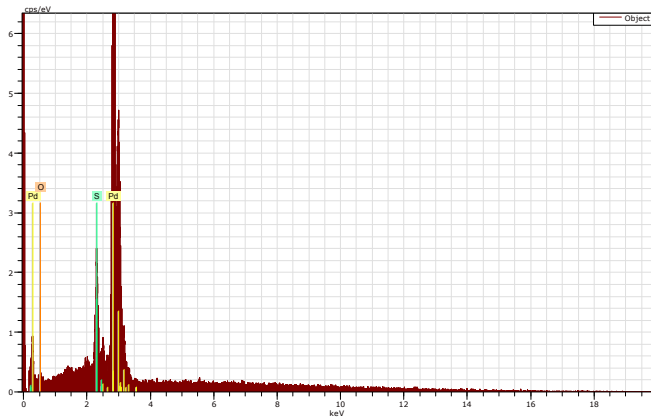


Figure S22. EDX pattern of the prismatic Pd_{16}S_7 nanoparticles.

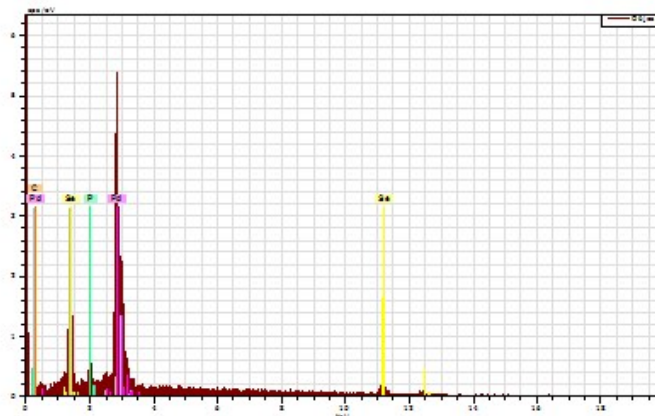


Figure S23. EDX pattern of the prismatic $\text{Pd}_{17}\text{Se}_{15}$ nanoparticles.

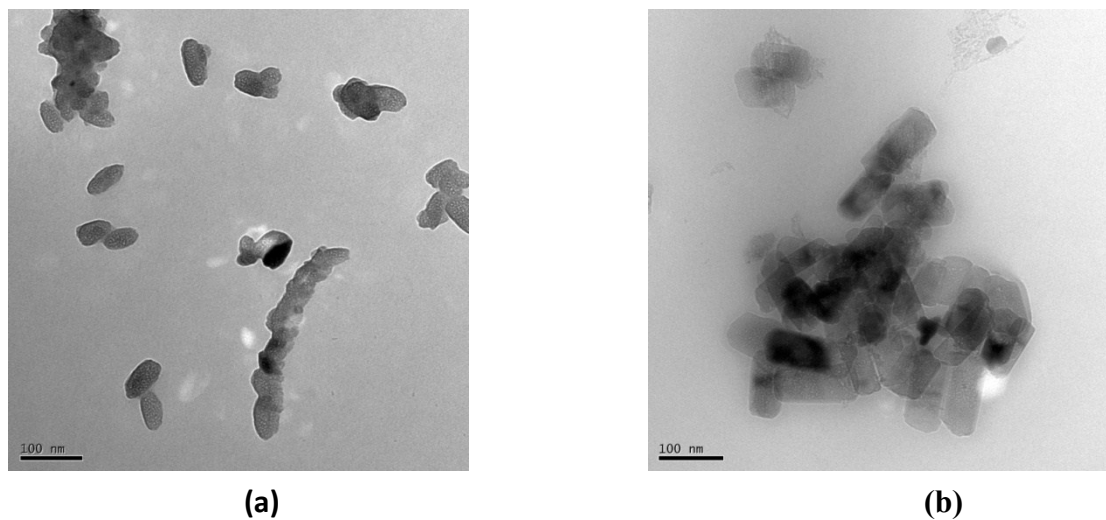


Figure S24. TEM Images of (a) Pd_{16}S_7 NPs (Scale Bar 100 nm). (b) $\text{Pd}_{17}\text{Se}_{15}$ NPs (Scale Bar 100 nm) after 4 Run Cycle .

Proposed mechanism for Suzuki-Miyaura coupling

The mechanism for Suzuki–Miyaura coupling reaction, where Pd_{16}S_7 and $\text{Pd}_{17}\text{Se}_{15}$ NPs are catalytic species is shown in Fig. S25. It based on earlier proposed pathway.²

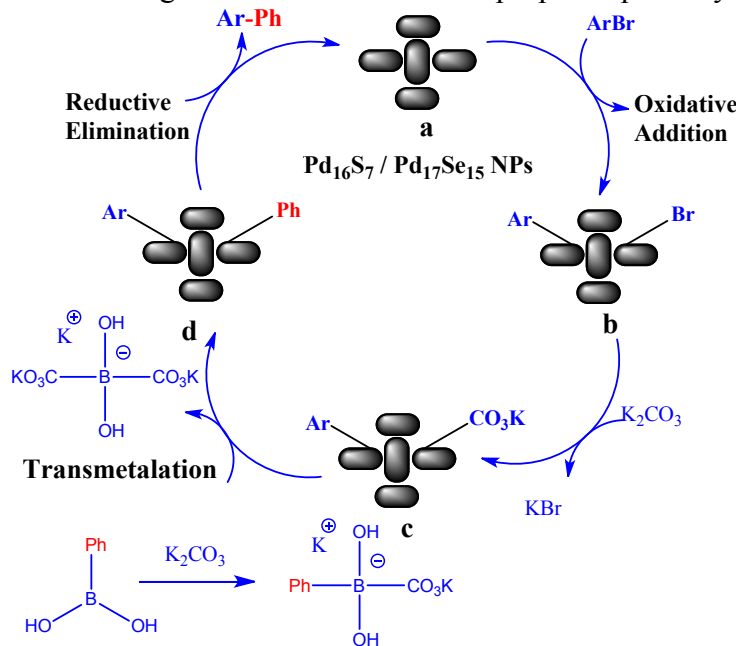


Figure S25. Mechanism for Suzuki–Miyaura coupling reactions.

Proposed Mechanism for C–O coupling

The mechanism for C–O coupling reaction catalyzed with Pd_{16}S_7 / $\text{Pd}_{17}\text{Se}_{15}$ NPs is proposed on the basis of earlier reports³ and is shown in Fig. S26. It is based on Pd(0).

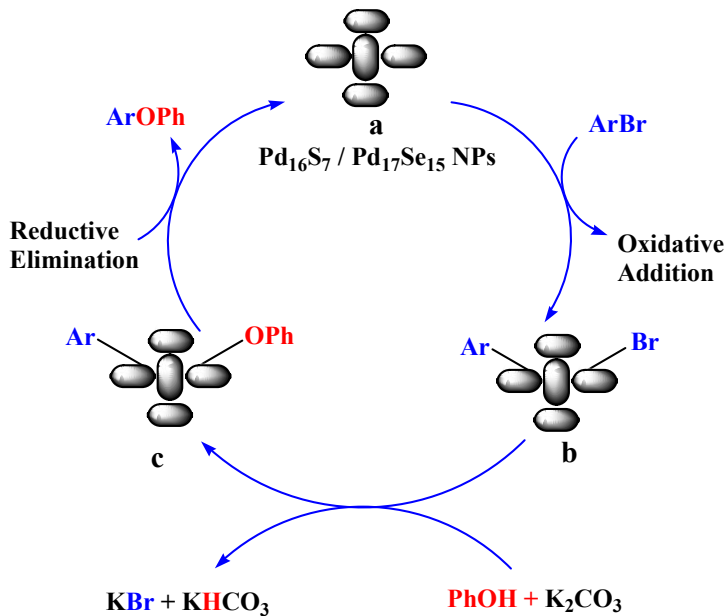


Figure S26. Mechanism for C–O coupling reactions.

Table S6. Optimization of conditions for Suzuki–Miyaura cross coupling reaction catalyzed with Pd_{16}S_7 / $\text{Pd}_{17}\text{Se}_{15}$ NPs^a

S. No.	Catalyst ^a	Solvent	Base	Time (h)	Conversion (%)
1.	Pd_{16}S_7 / $\text{Pd}_{17}\text{Se}_{15}$	DMF (4 mL)	K_2CO_3	12	81/75
2.	Pd_{16}S_7 / $\text{Pd}_{17}\text{Se}_{15}$	DMF (4 mL)	Cs_2CO_3	12	55/58
3.	Pd_{16}S_7 / $\text{Pd}_{17}\text{Se}_{15}$	Toluene (4 mL)	CH_3ONa	12	44/45
4.	Pd_{16}S_7 / $\text{Pd}_{17}\text{Se}_{15}$	EtOH (4 mL)	K_2CO_3	12	38/40
5.	Pd_{16}S_7 / $\text{Pd}_{17}\text{Se}_{15}$	H_2O (4 mL)	K_2CO_3	12	12/< 10
6.	Pd_{16}S_7 / $\text{Pd}_{17}\text{Se}_{15}$	DMF: H_2O (3:1 mL)	Cs_2CO_3	12	68/70
7.	Pd_{16}S_7 / $\text{Pd}_{17}\text{Se}_{15}$	DMF: H_2O (3:1 mL)	K_2CO_3	12	100/100
8.	Pd_{16}S_7 / $\text{Pd}_{17}\text{Se}_{15}$	DMF: H_2O (3:1 mL)	K_2CO_3	6	100/100
9.	Pd_{16}S_7 / $\text{Pd}_{17}\text{Se}_{15}$	DMF: H_2O (3:1 mL)	K_2CO_3	3	90/96
10.	Pd_{16}S_7 / $\text{Pd}_{17}\text{Se}_{15}$	DMF: H_2O (3:1 mL)	K_2CO_3	1	61/68
11.	Pd_{16}S_7 / $\text{Pd}_{17}\text{Se}_{15}^*$	DMF: H_2O (3:1 mL)	K_2CO_3	1	65/72
12.	Pd_{16}S_7 / $\text{Pd}_{17}\text{Se}_{15}$	EtOH: H_2O (3:1 mL)	K_2CO_3	12	42/50

^aReaction conditions: 4-bromobenzaldehyde (1.0 mmol), phenylboronic acid (1.5 mmol), base (2.0 mmol), Pd_{16}S_7 / $\text{Pd}_{17}\text{Se}_{15}$ nanoparticles: 0.5 mol % of Pd, temp. 100 °C. Conversion: ¹H NMR based. * Pd_{16}S_7 / $\text{Pd}_{17}\text{Se}_{15}$ NPs equivalent to 1.0 mol % of Pd.

Table S7. Optimization of Conditions for C–O Coupling Reaction Catalyzed with $\text{Pd}_{16}\text{S}_7/\text{Pd}_{17}\text{Se}_{15}$ NPs^a

Pd₁₆S₇ / Pd₁₇Se₁₅ NPs
K₂CO₃, DMSO

S. No.	Catalyst ^a	Solvent	Base	Time (h)	Conversion (%)
1.	Pd ₁₆ S ₇ / Pd ₁₇ Se ₁₅	DMF (4 mL)	K ₂ CO ₃	12	42/45
2.	Pd ₁₆ S ₇ / Pd ₁₇ Se ₁₅	DMF(4 mL)	Cs ₂ CO ₃	12	24/30
3.	Pd ₁₆ S ₇ / Pd ₁₇ Se ₁₅	DMF (4 mL)	NaO'Bu	12	19/25
4.	Pd ₁₆ S ₇ / Pd ₁₇ Se ₁₅	DMSO (4 mL)	K ₂ CO ₃	12	85/88
5.	Pd ₁₆ S ₇ / Pd ₁₇ Se ₁₅	DMSO (4 mL)	Cs ₂ CO ₃	12	59/65
6.	Pd ₁₆ S ₇ / Pd ₁₇ Se ₁₅	DMSO (4 mL)	K ₂ CO ₃	6	82/85
7.	Pd ₁₆ S ₇ / Pd ₁₇ Se ₁₅	DMSO (4 mL)	K ₂ CO ₃	3	80/85
8.	Pd ₁₆ S ₇ / Pd ₁₇ Se ₁₅	DMSO (4 mL)	K ₂ CO ₃	1	55/58
9.	Pd ₁₆ S ₇ / Pd ₁₇ Se ₁₅	ETOH (4 mL)	K ₂ CO ₃	12	29/35
10.	Pd ₁₆ S ₇ / Pd ₁₇ Se ₁₅	ETOH (4 mL)	Cs ₂ CO ₃	12	22/30

^aReaction conditions: 4-bromobenzaldehyde (1.0 mmol), phenol (1.1 mmol), base (2.0 mmol), $\text{Pd}_{16}\text{S}_7/\text{Pd}_{17}\text{Se}_{15}$ NPs: 0.5 mol % of Pd, temp. 100 °C. Conversion: ¹H NMR based.

Table S8. Optimization of base, solvent and time for Suzuki–Miyaura coupling reaction catalyzed with **C1/C2**.

S. No.	Catalyst ^a	Solvent	Base	Time (h)	Conversion (%)
1.	C1/C2	DMF (4 mL)	K ₂ CO ₃	12	79/72
2.	C1/C2	DMF (4 mL)	Cs ₂ CO ₃	12	61/58
3.	C1/C2	Toluene (4 mL)	CH ₃ ONa	12	48/46
4.	C1/C2	EtOH (4 mL)	K ₂ CO ₃	12	35/37
5.	C1/C2	H ₂ O (4 mL)	K ₂ CO ₃	12	28/21
6.	C1/C2	EtOH : H ₂ O (3 : 1 mL)	K ₂ CO ₃	12	45/39
7.	C1/C2	DMF : H ₂ O (3 : 1 mL)	Cs ₂ CO ₃	12	73/72
8.	C1/C2	DMF : H ₂ O (3 : 1 mL)	K ₂ CO ₃	12	100/100
9.	C1/C2	DMF : H ₂ O (3 : 1 mL)	K ₂ CO ₃	3	100/100
10.	C1/C2	DMF : H ₂ O (3 : 1 mL)	K ₂ CO ₃	2	100/97

^aReaction conditions: 4-bromobenzaldehyde (1.0 mmol), phenylboronic acid (1.5 mmol), base (2.0 mmol), **C1 / C2** (0.01 mol %), temp. 100 °C, Conversion: ¹H NMR based.

Table S9. Optimization of base, solvent and time for C–O coupling reaction catalyzed with **C1/C2**.

S. No.	Catalyst ^a	Solvent	Base	Time (h)	Conversion (%)
1.	C1/C2	DMF (4 mL)	K ₂ CO ₃	12	44/39
2.	C1/C2	DMF(4 mL)	Cs ₂ CO ₃	12	32/21
3.	C1/C2	DMF (4 mL)	NaO'Bu	12	24/19
4.	C1/C2	DMSO (4 mL)	K ₂ CO ₃	12	98/79
5.	C1/C2	DMSO (4 mL)	Cs ₂ CO ₃	12	62/55
6.	C1/C2	DMSO (4 mL)	K ₂ CO ₃	6	95/75
7.	C1/C2	DMSO (4 mL)	K ₂ CO ₃	3	95/72
8.	C1/C2	DMSO (4 mL)	K ₂ CO ₃	1	80/59
9.	C1/C2	ETOH (4 mL)	K ₂ CO ₃	12	31/26
10.	C1/C2	ETOH (4 mL)	Cs ₂ CO ₃	12	29/28

^aReaction conditions: 4-bromobenzaldehyde (1.0 mmol), phenol (1.1 mmol), base (2.0 mmol), **C1** 0.1 mol %, temp. 100 °C. Conversion: ¹H NMR based.

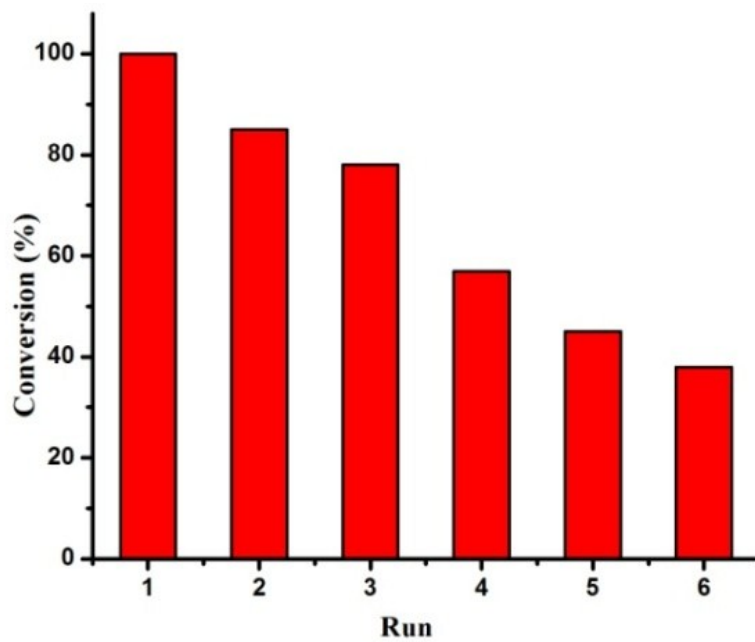


Figure S27. ‘Catalyst Alive’ Test for SMC of 4-Bromobenzaldehyde, Catalyst 0.001 mol%.

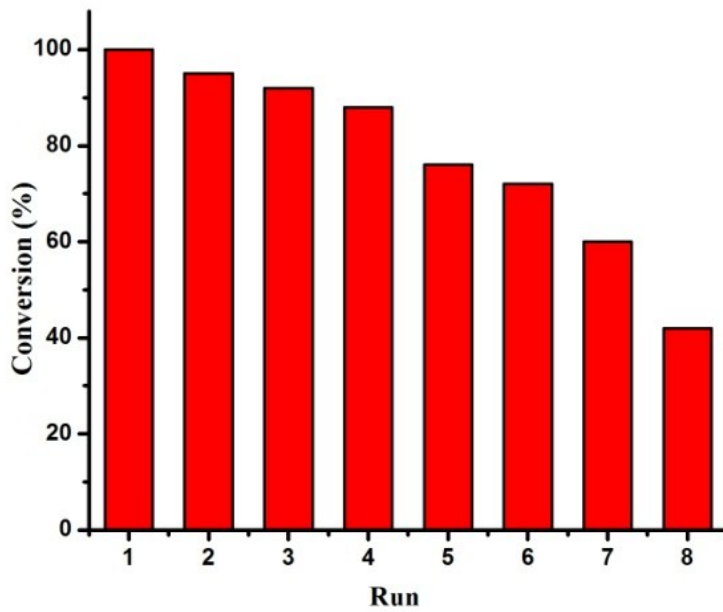


Figure S28. ‘Catalyst Alive’ Test for C–O Coupling of 1-Bromo-4-nitrobenzene, Catalyst 0.1 mol%.

C–C couplin reaction.^{4,5}

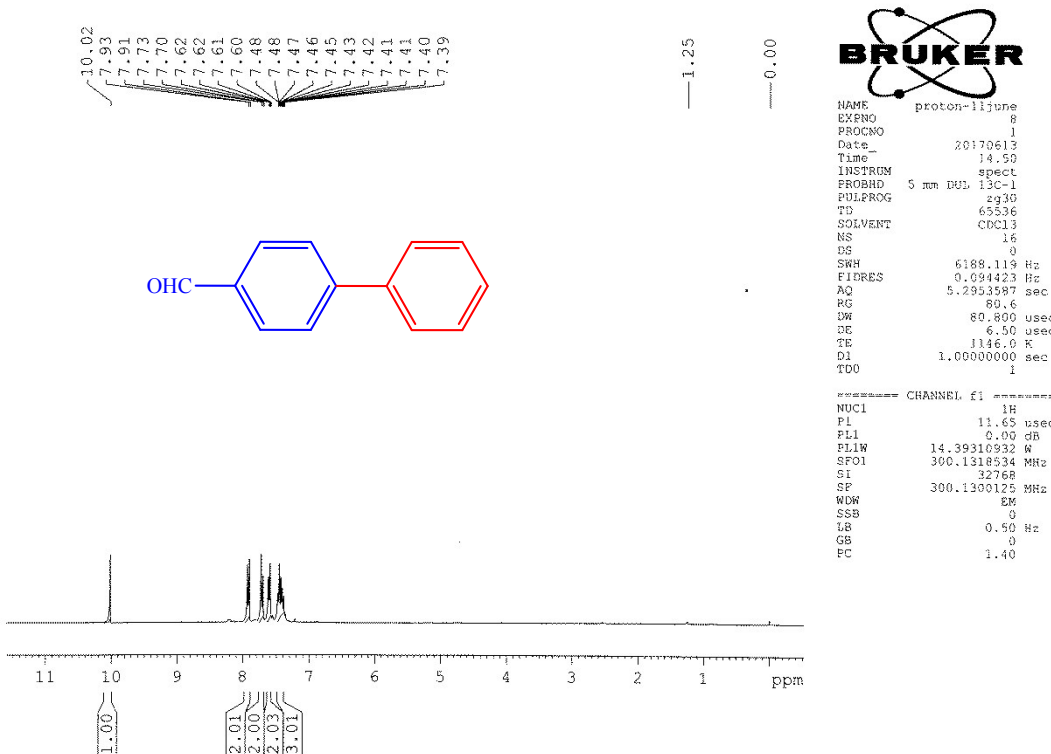


Figure S29. ¹H NMR of 4-Phenylbenzaldehyde

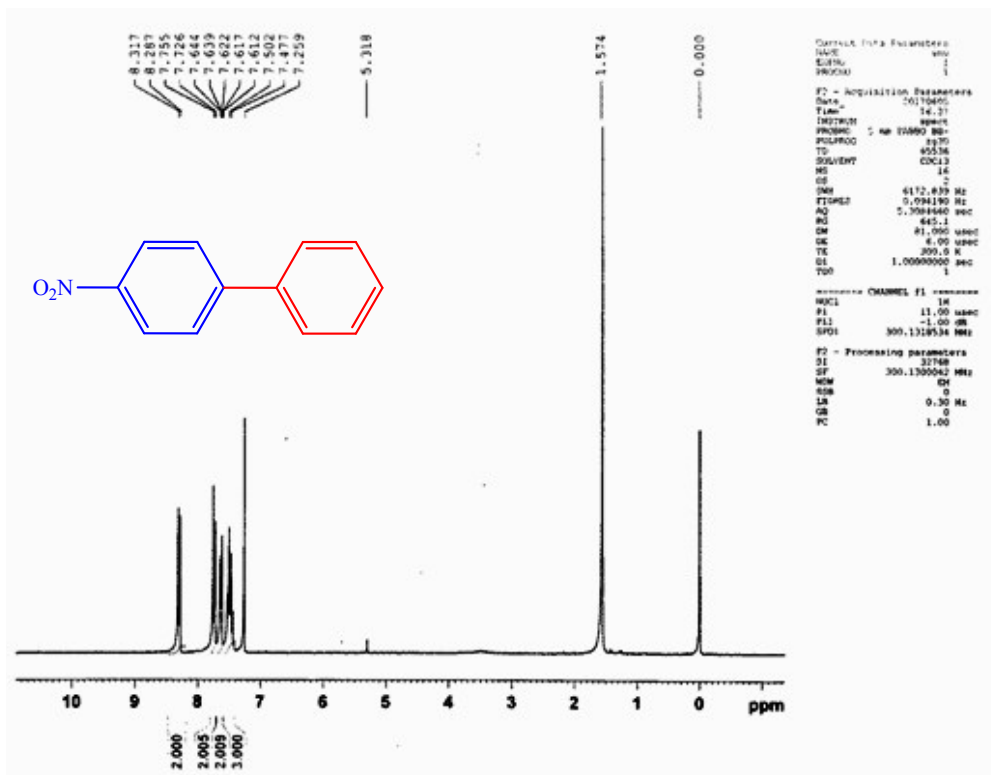


Figure S30. ¹H NMR of 4-Nitrobiphenyl

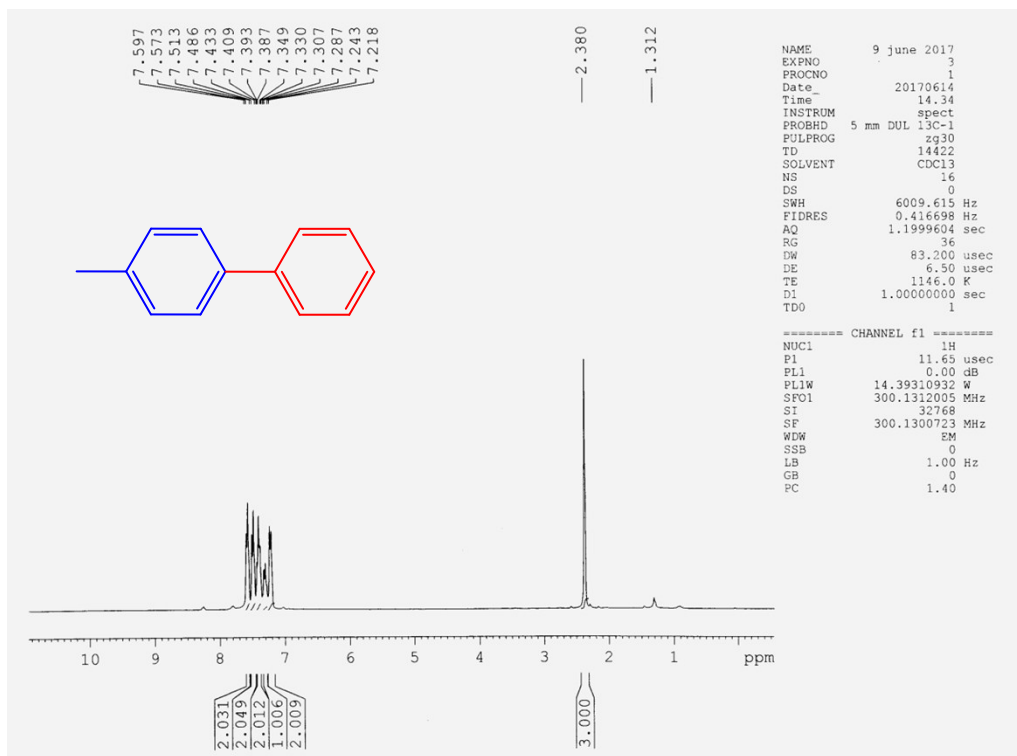


Figure S31. ¹H NMR of 4–Methylbiphenyl

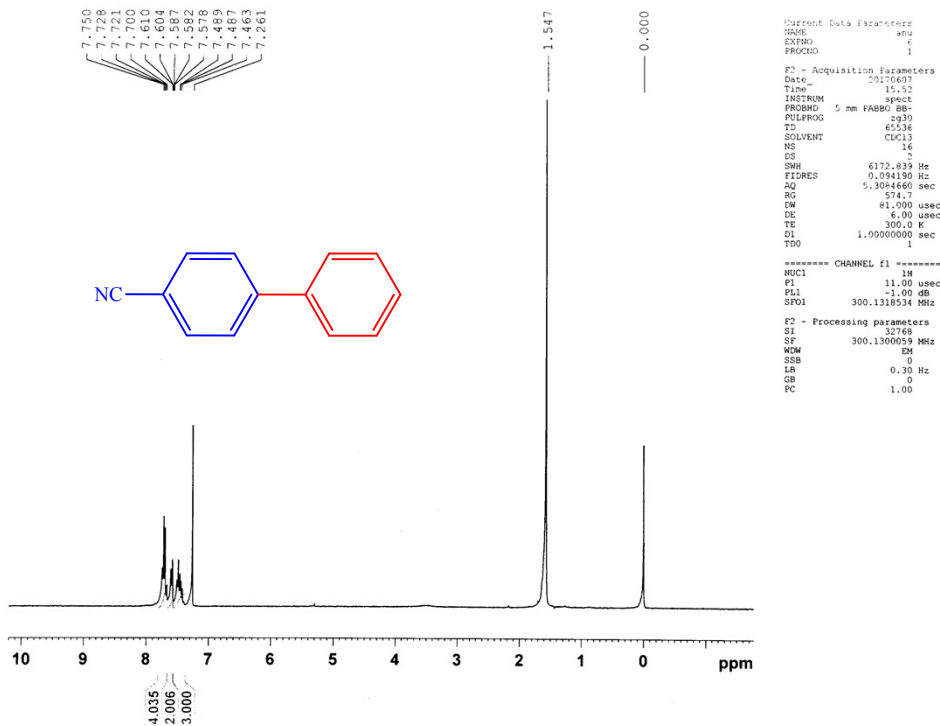


Figure S32. ¹H NMR of 4–Phenylbenzonitrile

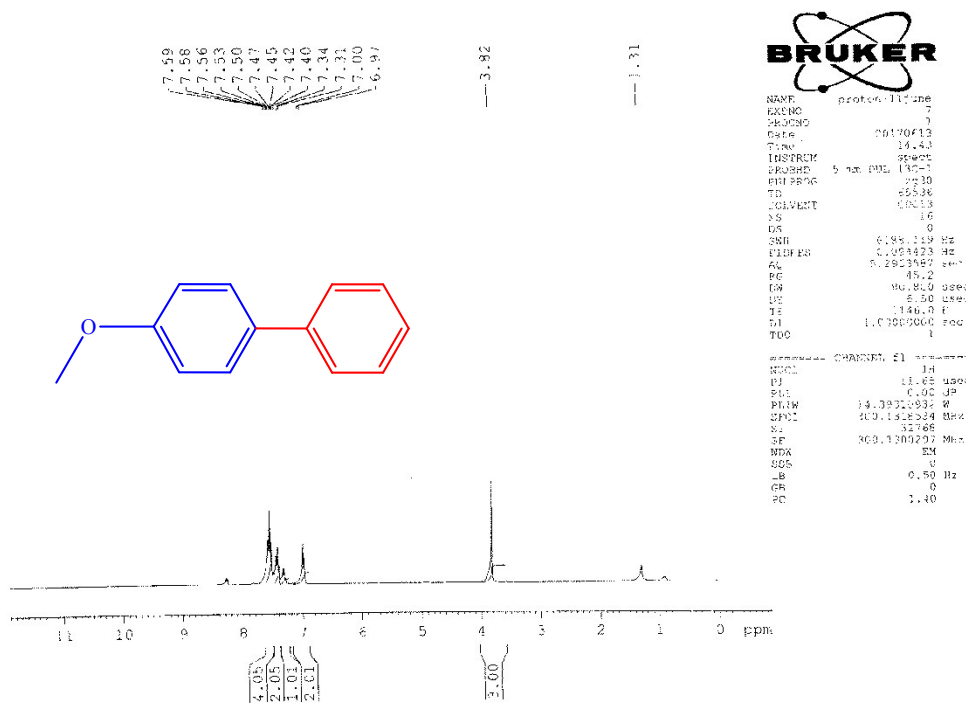


Figure S33. ^1H NMR of 4-Methoxybiphenyl

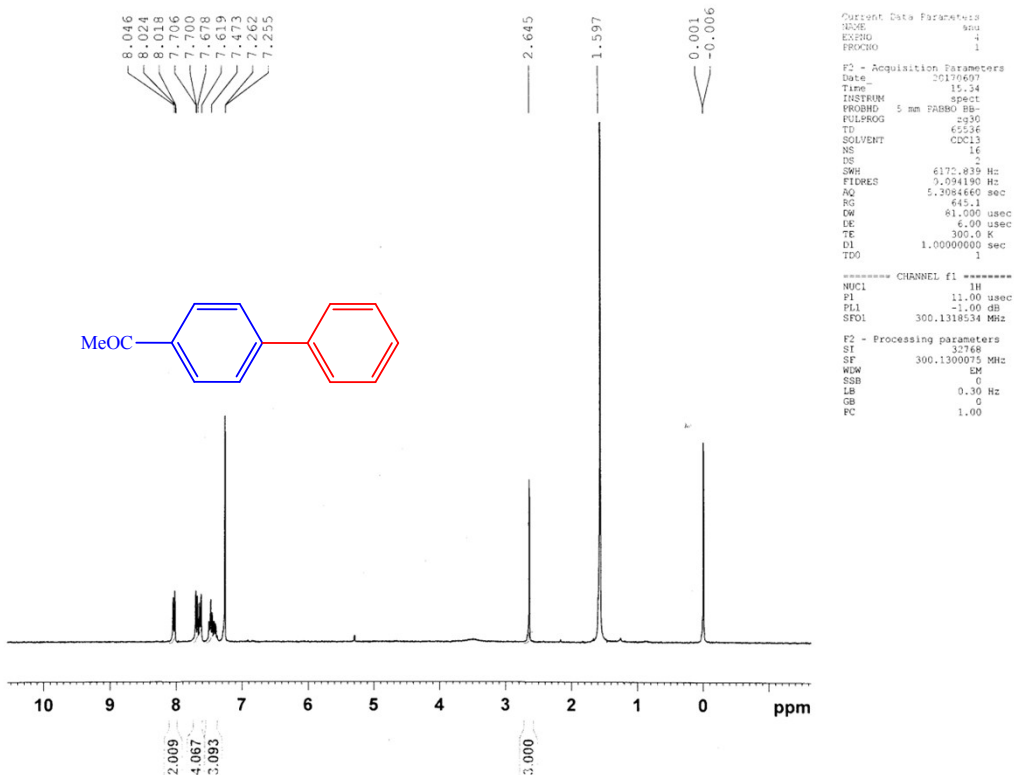


Figure S34. ^1H NMR of 4-Acetyl biphenyl

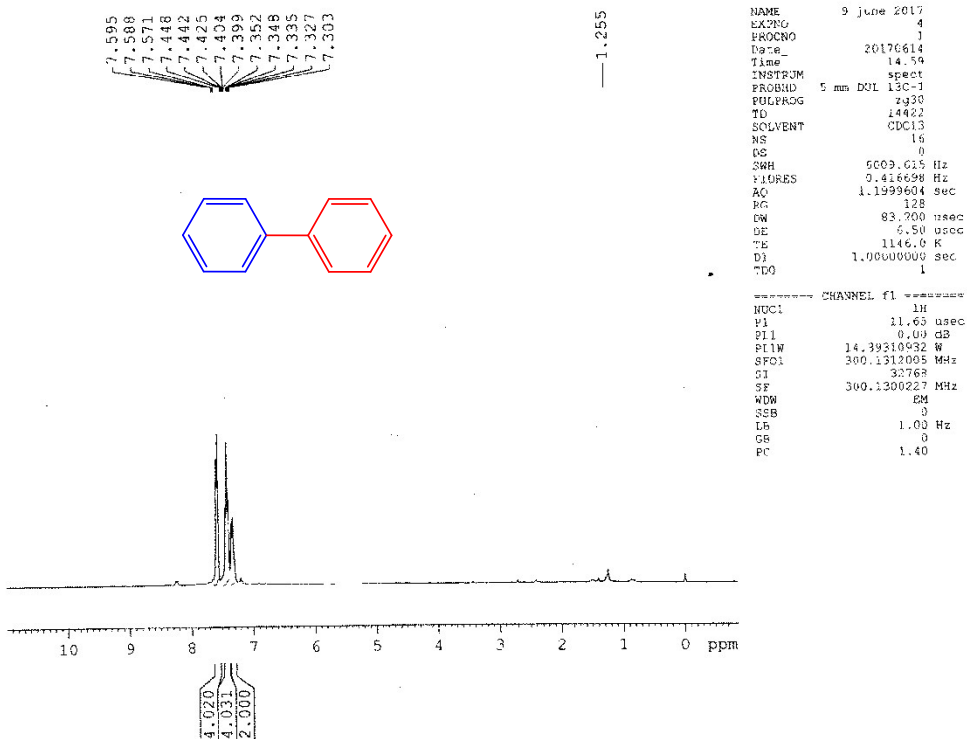


Figure S35. ^1H NMR of Biphenyl

C–O coupling reaction.^{6,7}

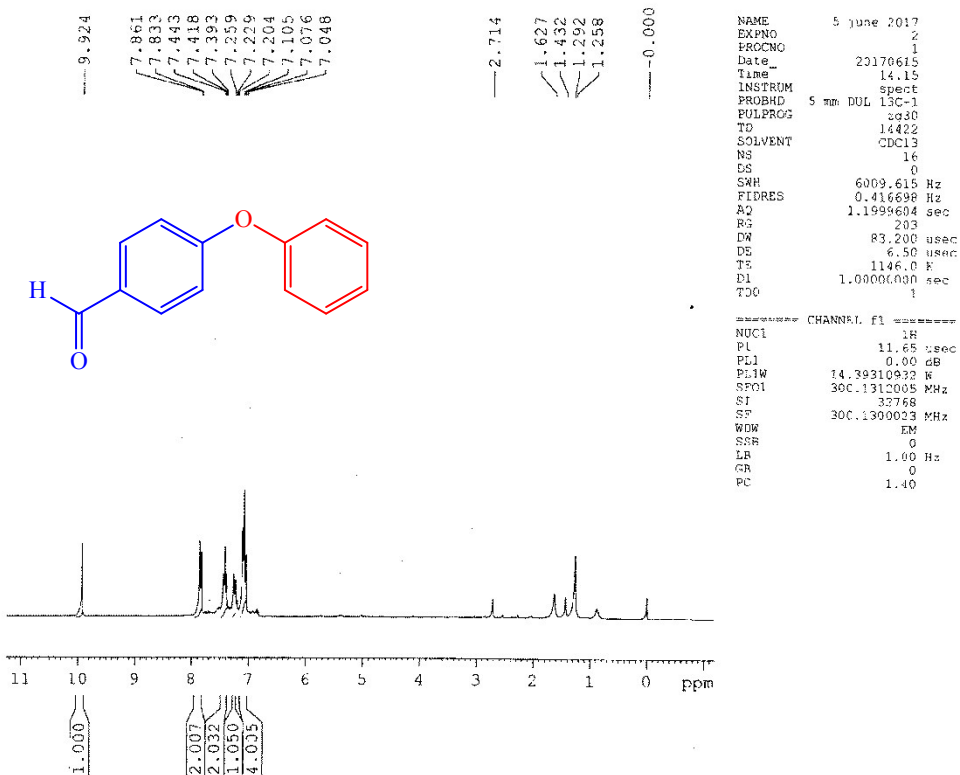
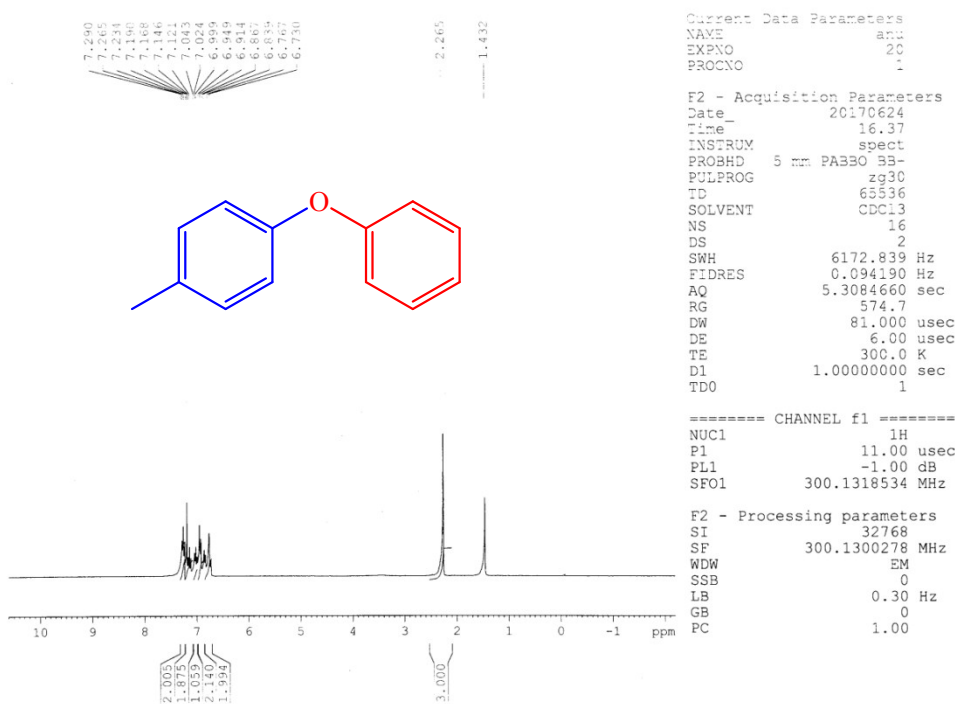
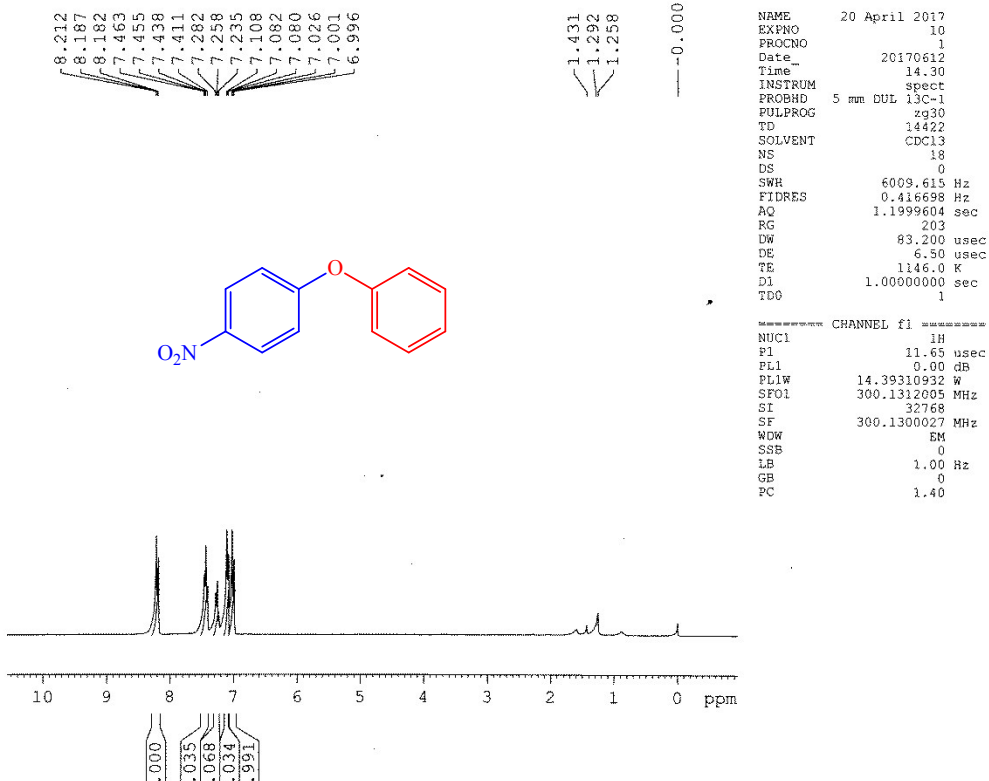


Figure S36. ^1H NMR of 4–phenoxybenzaldehyde



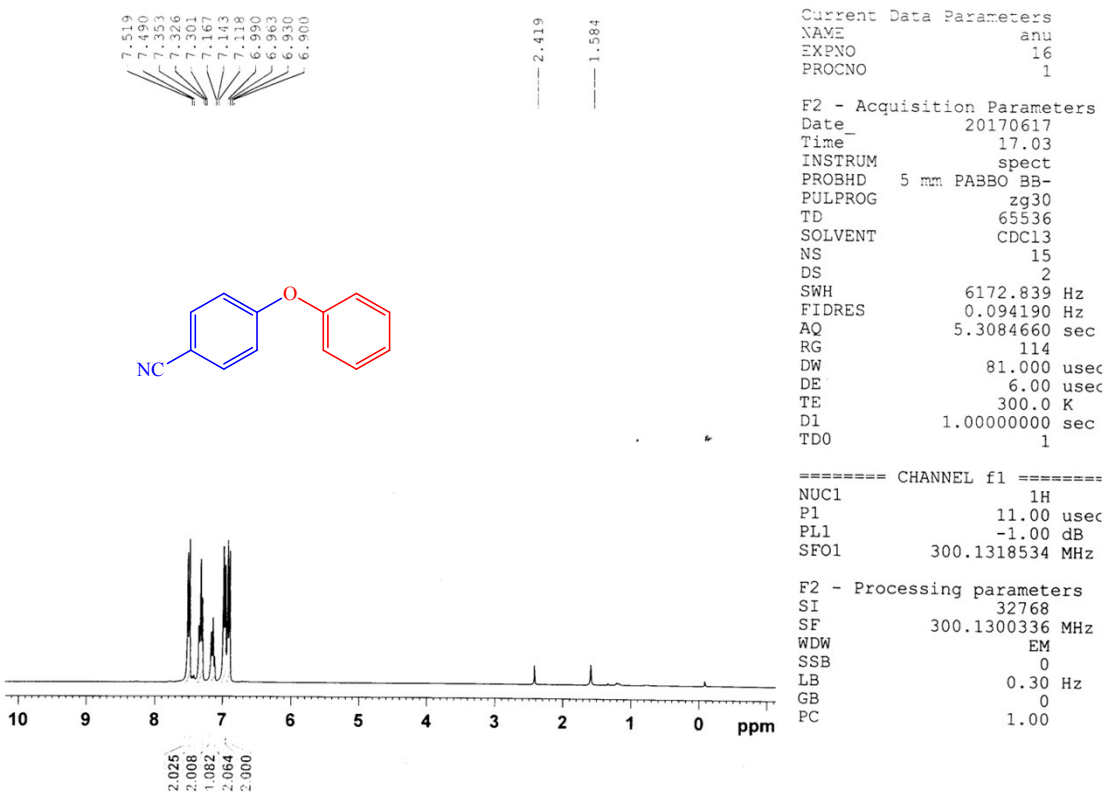


Figure S39. ^1H NMR of 4-phenoxybenzonitrile

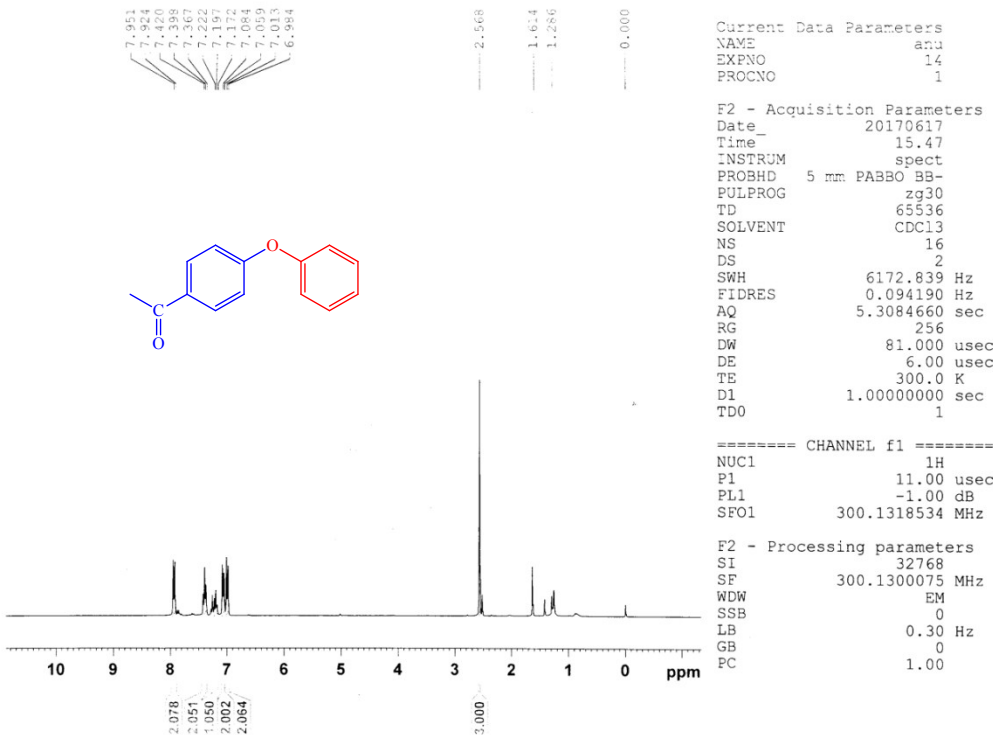


Figure S40. ^1H NMR of 1-(4-phenoxyphenyl)ethanone

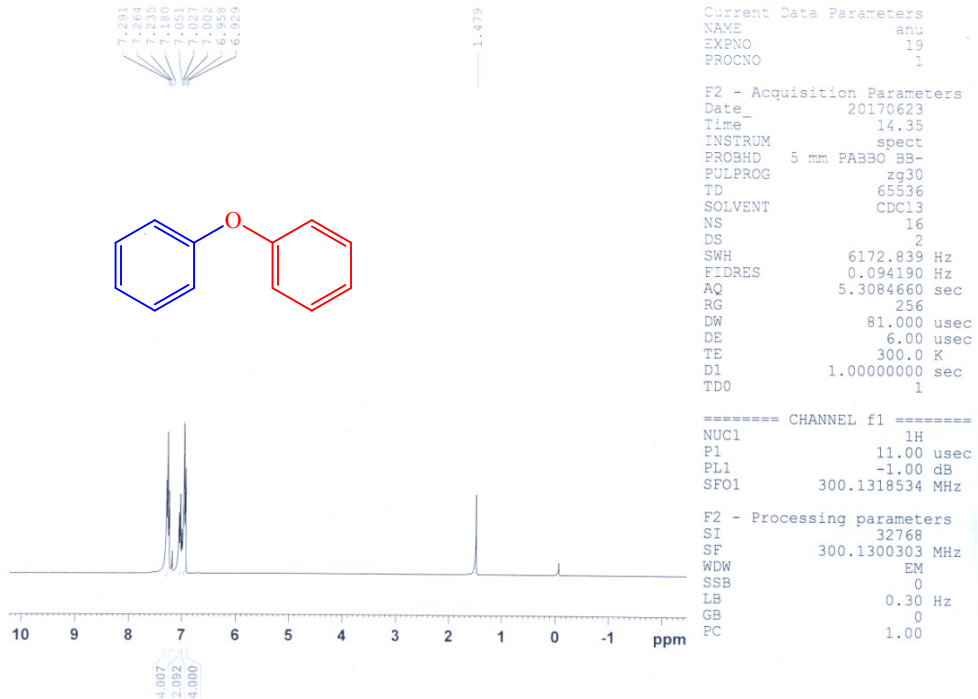


Figure S41. ¹H NMR of Diphenyl ether

References

- (a) P. Singh, A. K. S. Chauhan, R. J. Butcher and A. Duthie, *J. Organomet. Chem.*, 2013, **728**, 44. (b) P. Singh, A. K. S. Chauhan, R. J. Butcher and A. Duthie, *J. Organomet. Chem.*, 2013, **731**, 49. (c) A. K. S. Chauhan, P. Singh, R. C. Srivastava, R. J. Butcher and A. Duthie, *J. Organomet. Chem.*, 2011, **696**, 3649. (d) A. K. S. Chauhan, P. Singh, R. C. Srivastava, R. J. Butcher and A. Duthie, *J. Organomet. Chem.*, 2010, **695**, 2532.
- (a) M. Pérez-Lorenzo, *J. Phys. Chem. Lett.*, 2012, **3**, 167. (b) B. Cornelio, A. R. Saunders, W. A. Solomonsz, M. Laronze-Cochard, A. Fontana, J. Sapi, A. N. Khlobystovcd and G. A. Rance, *J. Mater. Chem. A*, 2015, **3**, 3918. (c) P. Purohit, K. Seth, A. Kumar and A. K. Chakraborti, *ACS Catal.*, 2017, **7**, 2452.
- (a) A. Aranyos, D. W. Old, A. Kiyomori, J. P. Wolfe, J. P. Sadighi and S. L. Buchwald, *J. Am. Chem. Soc.*, 1999, **121**, 4369. (b) K. E. Torracca, X. Huang, C. A. Parrish and S. L.

- Buchwald, *J. Am. Chem. Soc.*, 2001, **123**, 10770. (c) S. Gowrisankar, A. G. Sergeev, P. Anbarasan, A. Spannenberg, H. Neumann and M. Beller, *J. Am. Chem. Soc.*, 2010, **132**, 11592. (d) G. L Tolnai, B. Pethő, P. Králl and Z. Novák, *Adv. Synth. Catal.*, 2014, **356**, 125. (e) T. M. Rangarajan, R. Singh, R. Brahma, K. Devi, R. P. Singh, R. P. Singh and A. K. Prasad, *Chem. Eur. J.*, 2014, **20**, 14218.
4. B. Tao, D. W. Boykin, *J. Org. Chem.*, **2004**, *69*, 4330– 4335.
 5. R. K. Arvela, N. E. Leadbeater, *Org. Lett.*, **2005**, *7*, 2101–2104.
 6. T. Hu, T. Schulz, C. Torborg, X. Chen, J. Wang, M. Beller, J. Huang, *Chem. Commun.*, **2009**, 7330–7332.
 7. Q. Zhang, D. Wang, X. Wang, K. Ding, *J. Org .Chem.*, **2009**, *74*, 7187–7190.